

DESIGN OF LOW SPEED AXIAL FLUX PERMANENT
MAGNET GENERATORS FOR MARINE CURRENT
APPLICATION

SANJIDA MOURY



Design of Low Speed Axial Flux Permanent Magnet Generators for Marine Current Application

A thesis presented to the school of Graduate Studies of Memorial University of
Newfoundland in Partial fulfillment of the requirement leading to the award of a Master
of Engineering in
ELECTRICAL ENGINEERING

By

© SANJIDA MOURY

Department of Electrical Engineering
Faculty of Engineering & Applied Science
Memorial University of Newfoundland

October 7, 2009

Dedication

I would like to dedicate my thesis to my beloved parents

Abstract

The aim of this research work is to design, built and test low speed multiploe permanent magnet generators for ocean energy conversion systems. Vertical axis drag/lift type ocean current turbines have low speed due to water speed of less than 1m/s. A low speed permanent magnet generator can be utilized to deliver low power that can be used to power- rated sea pods. The study focuses on the design of a permanent magnet generator, which is suitable for under water application and can generate electric power from the low speed marine currents (typically below 100rpm). This thesis explores different low speed permanent magnet generators and focuses on multipole direct driven axial flux permanent magnet Generator (AFPMG). AFPMG is suitable for direct coupled systems. Two types of AFPMG are designed and tested for several performance criterions. The prototyped AFPMGs are tested and the results are presented and discussed in this thesis. The first design produced 5.2V, 3.5W and the second design produced about 5.5V, 2W at 70 rpm. Both designs are simple in construction, economically viable and suitable for low electric power generation from ocean currents.

Acknowledgements

By the name of Almighty Allah

This thesis arose in part out of years of research that has been done since I came to Seaformatics group. This research has been supported by Atlantic Innovation Fund and Seaformatics. I have worked with a great number of people whose contribution in assorted ways to the research and the making of the thesis deserved special mention. It is a pleasure to convey my gratitude to them all in my humble acknowledgment.

In the first place I would like to record my gratitude to my supervisor, Dr. Tariq Iqbal for his supervision, advice, and guidance from the very early stage of this research as well as giving me extraordinary experiences through out the work. Above all and the most needed, he provided me unflinching encouragement and support in various ways. His truly scientist intuition has made him as a constant oasis of ideas and passions in science, which exceptionally inspire and enrich my growth as a student, a researcher and a scientist want to be. I am indebted to him more than he knows.

I gratefully acknowledge Dr. V. Masek for his advice and encouragement. Many thanks go in particular to Paul Bisop and Brian pretty. Paul went far beyond the call of duty to help me design and fabricate my prototype. I had the opportunity to meet and work with this two great individuals and I learnt a lot from them.

All members of Technical service who paid a lot of time and effort to build the prototype. Their helping attitude towards me will be always memorable to me. A gratefully thank to Tom Pike and Grage Olery. They are always there to offer technical

support. A grateful acknowledges Phil Bonna for his computer support. How can I forget Crocker Moya, who was always with her smiling face and solution of all official problems? It is a pleasure to pay tribute also to all of the faculty members, official and technical staff who helped me at any context.

I gratefully thank Razzaqul Ahsan for his constructive comments on this thesis. It is a pleasure to pay tribute also to the Nahid Sultana, Nigar Sultana and my little two angles Labib and Romin, without them my life in Canada is boring and friendless. Also thanks to Nahidul Islam Khan, Rousseau Zubayer, Sejuti Baral, Sanjala Rizvan Nashin and Israt Zahan for their encouragement. I would like to pay my gratitude to all of my friends in Bangladesh who always encourage me in different context.

Where would I be without my family? My parents, who sincerely raised me with their caring and gently love, deserve special mention for their inseparable support and prayers. Thanks dad (Abdul Wahab Khan) for always to be with me. My Mother, Mushahida Begum, in the first place is the person who put the fundament my learning character, showing me the joy of intellectual pursuit ever since I was a child. I was extraordinarily fortunate in having such a nice sister Wahida Barnaly who is always beside me with encouragement and love.

Finally, I would like to thank everybody who was important to the successful realization of thesis, as well as expressing my apology that I could not mention personally one by one.

Table of figures

Figure 1.1: Permanent magnet machine (a) radial flux (b) axial flux	5
Figure 1.2: Single sided AFPM machine	7
Figure 1.3: Double sided AFPM machine (a) internal rotor (b) internal stator	8
Figure 1.4: Multidisk AFPM machine	9
Figure 1.5: Interior magnet rotor.....	10
Figure 1.6: Surface magnet rotor.....	11
Figure 1.7: Inset magnet rotor.....	11
Figure 1.8: Buried magnet rotor.....	12
Figure 1.9: AFPM disc-type motor structures: (a) slotless TORUS, (b) slotted TORUS, (c) slotless AFIR, and (d) slotted AFIR machines.....	13
Figure 1.10: Three-dimensional (3-D) flux paths of the (a) TORUS and (b) AFIR type topologies.....	13
Figure 3.1: Axial flux permanent magnet generator: (a) TORUS Topology (b) NN type (c) NS type.....	39
Figure 3.2: Two pole section of (a) conventional double rotor single stator TORUS machine with the same magnet pole-arc and (b) TORUS machine with alternating pole arcs	40
Figure 3.3: Simplified Cross section of a rotor with shifted magnets.....	41
Figure 3.4: The first prototyped generator	42
Figure 3.5: Permanent magnet (a) Larger (b) Smaller.....	45
Figure 3.6: The rotor (a) full view with magnets (b) sectional view.....	46

Figure 3.7: E-Core with dimensions.....	47
Figure 3.8: The stator (a) solid works design (b) stator with E-core (c) Stator with winding.....	47
Figure 3.9: A sectional view of prototyped generator.....	48
Figure 3.10: Initial torque measurement.....	53
Figure 3.11: Test setup for first prototype.....	53
Figure 3.12: Open circuit characteristic of first prototype.....	54
Figure 3.13: Output characteristic of first prototype.....	54
Figure 3.14 load current and voltage of first prototype	55
Figure 3.15 Power curve of first prototype.....	55
Figure 3.16: The waveform of the first prototyped generator (a) individual wave form of the both side of the stator (b) the resultant waveform of the generator after adding two stators in series.....	57
Figure 3.17: Simplified system model of Generator.....	58
Figure 4.1: PCB board.....	63
Figure 4.2: A 2D view of the double sided AFPMG with PCB stator.....	64
Figure 4.3: The prototyped generator.....	64
Figure 4.4: Isometric view of the rotor	65
Figure 4.5: 3D view of the magnet with dimensions	65
Figure 4.6: The spacing between the magnets.....	66
Figure 4.7: Final view of the rotor with magnets.....	66
Figure 4.8: The prototyped rotor.....	66
Figure 4.9: The PCB stator.....	68

List of Tables

TABLE 3.1 Selected Magnet properties.....	43
TABLE 3.2 RENSHAPE material properties.....	45
TABLE 3.3 Properties of AWG 20.....	48
TABLE 3.4: Generator design parameters.....	49
TABLE 3.5: Generator parameters.....	58
TABLE 4.1: Rotor Yoke (mild steel C-1020) data.....	66
TABLE 4.2: FR-4 data.....	67
TABLE 4.3: Generator design parameters.....	69
TABLE 4.4: Generator parameters.....	77

Contents

ABSTRACT.....	iii
ACKNOWLEDGEMENT.....	iv
List of Figures.....	vi
List of Tables.....	ix
CHAPTER 1- INTRODUCTION	
1.1. Background.....	1
1.2. Permanent Magnet Machine.....	4
1.3. Axial Flux Generator.....	6
1.3.1. Geometries.....	6
1.3.1.1. Single Sided Machine	6
1.3.1.2. Double Sided Machine.....	7
1.3.1.3. Ironless Double Sided Machine.....	8
1.3.1.4. Multidisk Machine.....	9
1.3.1.5. Rotor Configuration.....	9
1.3.2. Axial Flux Disk Type Structure.....	12
1.3.3. Performance Characteristics.....	15
1.3.3.1. Cogging Torque.....	15
1.3.3.2. Pulsating Torque.....	17

1.4. Permanent Magnet Material.....	18
1.4.1. History.....	18
1.4.2. PM Material.....	20
CHAPTER 2- REVIEW OF RELATED WORKS.....	24
2.1. Comparison of PM Generators.....	24
2.2. PM Axial Flux Generator.....	26
2.3. Minimization of Cogging Torque.....	28
2.4. Ironless Stator Axial Flux Permanent Magnet Machine.....	29
2.5. Conclusion.....	31
CHAPTER 3- FIRST PROTOTYPE PMG.....	33
3.1. Background.....	33
3.2. Design Challenges.....	34
3.3. Design Topology for Minimizing Cogging Torque.....	36
3.3.1. The TORUS Configuration.....	37
3.3.2. Alternating Pole Arc.....	38
3.3.3. Magnet Shifting.....	39
3.3.4. Fractional Number of Slots.....	40
3.4. Design.....	40
3.4.1. Permanent Magnet.....	41
3.4.2. Number of Pole.....	42
3.4.3. Rotor.....	43

3.4.4. stator.....	45
3.4.5. stator winding.....	47
3.5. Calculated Result.....	48
3.6. Test Result.....	50
3.6.1. Mechanical Parameter Test.....	50
3.6.2. Electrical Parameter Test.....	52
3.7. Generator Model.....	55
3.8. Result Analysis.....	56
3.9. Conclusion.....	57
CHAPTER 4- SECOND PROTOTYPE PMG.....	58
4.1. Background.....	58
4.2. Design Challenges.....	60
4.3. Design.....	61
4.3.1. Rotor	62
4.3.2. PCB stator.....	65
4.3.3. Stator Winding.....	66
4.4. Calculated Result.....	67
4.5. Test Result.....	69
4.5.1. Stress and Strain Test.....	69
4.5.2. Mechanical Parameter Test.....	70
4.5.3. Electrical Parameter Test.....	71
4.6. Generator Model.....	75
4.7. Result Analysis.....	75

4.8. Conclusion.....	76
CHAPTER 5- CONCLUSION AND FUTURE WORK.....	77
5.1. Conclusion.....	77
5.2. Future Work.....	79

Bibliography

Chapter 1

1. Introduction

1.1 Background

One of series challenges for the world future is linked with continuous demand for energy. Energy is by far the largest merchandise in the world and an enormous amount of energy is extracted, distributed, converted and consumed in the global society. The global energy demand is continuously increasing. Today's global energy production is highly, in fact 83% [1] dependent on fossil fuel resources such as oil, gas and coal. These resources are limited and their use results in global warming due to emission of greenhouse gases like carbon dioxide. Interest in renewable energy has depended on the perceived risks of using fossil fuels. To provide a sustainable power production in future and at the same time be concerned about global warming, there is a growing demand for energy from renewable resources such as wind, geothermal, solar and ocean.

Oceans can be considered as one of abundant energy resource that can be exploited to contribute in a sustainable manner for meeting increasing global energy demands. The oceans, covering more than 75% of the Earth, have long been appreciated as a vast renewable resource. Several types of ocean energy sources with different origins (thermal energy and kinetic energy) exist. The most developed conversion systems concern: *tidal energy*, which mainly results from the gravitational fields of the moon and

the earth; *thermal energy* (Ocean Thermal Energy Conversion or OTEC), resulting directly from solar radiation; *marine currents*, caused by thermal and salinity differences in addition to tidal effects, and *ocean waves*, generated by the action of the winds blowing over the ocean surface. Other technologies, namely *salinity gradient* devices, are at a much lower level of development.

The ocean current resources still remain predominantly untapped. However, the physics behind ocean currents is very promising for energy conversion. A number of studies have been completed on the energy potential of marine currents but there have been few on the engineering requirements for utilization of this resource. Countries where theoretical studies and experimental projects took place are the UK, Italy, Canada, Japan, Russia, Australia and China in addition to the European Union. In Europe two prototypes are being developed partially funded by the European Commission.

Kinetic energy from the sea can be harnessed using relatively conventional techniques which are similar in principle to those for extracting energy from the wind. Though energy conversion from marine currents is quite similar to that of wind energy conversion but there are also several differences between them. The underwater placement of a marine current energy converter (MCEC) gives some advantages such as no noise disturbance for the public, low visual exposure and little use of land space but also adds some challenges like the need for water and salt proof technology, difficult and costly maintenance etc. Another characteristic is the difference in density, which results in a higher power density. The energy content of a marine current of only 1m/s is equivalent to a wind speed of 9m/s. A final characteristic to highlight is the relatively high degree of utilization, tidal streams are likely to have a utilization factor up to 40-50

% and currents of more constant nature are likely to have a utilization factor up to 80 % [2]. For wind power the corresponding utilization factor is usually between 25-30. The utilization factor is defined as the actual annual energy output divided by the theoretical maximum and is dependent on the rated power of the installed device [3] A high utilization factor is important to achieve an economically viable power production [4,5].

A present day typical and a new directly driven marine current power plant are designed. The electromechanical system of a hydro power plant usually consists of three main parts: turbine, gearbox and generator. Due to the low current velocities, a marine current turbine will experience low rotational speeds, typically below 100 rpm. In conventional hydro installation, the generator rotational speed is usually 1500 or 1800 rpm. This means that a gearbox is needed between the turbine and the generator. A standard asynchronous generator can be used and the constant speed operation is commonly used in this type of power plant. The generator can be connected directly to the grid, which results in a simple electrical system. However, the gearbox adds to the weight, generates noise, demands regular maintenance and increases losses. The aim of this research project is to create a generator well suited to the slow moving marine currents energy conversion system.

Using permanent magnet (PM) generators as low speed energy converters is very common. The low speed generator does not require step-up gearbox in power transmission between the turbine and the generator, which is typically required in conventional drive train. As the generator is directly driven by the turbine, it is commonly known as a direct drive generator. The marine current power plant can be simplified by eliminating the gear and by using a low-speed direct drive generator. Many disadvantages

avoided in gearless (directly coupled) marine current turbines. The noise caused mainly by a high rotational speed can be reduced. The advantages are also high overall efficiency due to a low cut-in speed and reliability, reduced weight and diminished need for maintenance. However, the diameter of a low-speed generator may be rather large because a great number of poles are needed in a low-speed machine. Due to the multi-pole structure, the total length of the magnetic path is short. The winding overhangs can also be shorter and stator resistive losses lower than those in a long pole pitch machine. The output frequency is usually lower than 50Hz, and a frequency converter is usually needed in low-speed applications. The converter makes it possible to use the machines in variable speed operation. The speed can be variable over a relatively wide range depending on the marine current conditions, and the turbines can extract maximum power at different flow rate. The advantages of the variable speed operation are, for instance, the reduction of the drive train, mechanical stresses, the improved output power quality and the increased energy capture.

1.2 Permanent Magnet Machine

A permanent magnet is classified as a “hard” magnetic material in which the domain orientation is permanently fixed by an externally applied magnetizing force. The term permanent magnet (or PM) machine is used herein to include all electromagnetic conversion devices in which the magnetic excitation is supplied by a permanent magnet (PM). PM machines compose a well-known class of rotating and linear electric machines used in both the motoring and generating modes. A PM generator consists of a stator with armature winding and a rotor mounted with permanent magnets to provide the field flux.

It does not need an external supply to excite the rotor field and hence the field winding and slip rings are eliminated.

There are many varying physical configurations for PM machines including radial (Fig. 1.1a) and axial (Fig. 1.1b) air gap configurations. In general, the use of PM excitation provides the machine designer with a greater degree of freedom in physical configuration than most other classes of rotating electric machines.

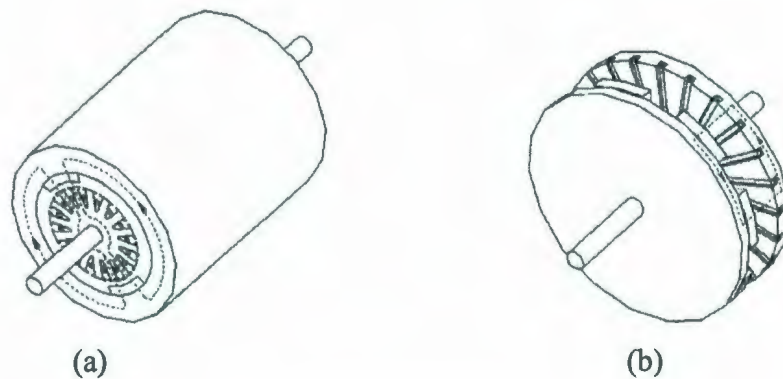


Figure 1.1: Permanent magnet machine (a) radial flux (b) axial flux

The rotor of a PM machine has a special design to give the required characteristics. Numerous rotor geometries of PM generator have been developed. Depending on the orientation of the magnetization, the rotor can be classified into two types, radially oriented type and circumferential type [6]. In radially oriented type, the rotor magnets are oriented such that the direction of magnet field of the permanent magnets in the machine is radial. Thus, the air gap flux density above the magnet is approximately the same as the magnetic flux density. This type of rotor construction using low residual flux density magnetic material such as ferrite magnets, results in very low air gap flux density. However, with the development of high-energy permanent magnets such as neodymium-

iron-boron (NdFeB) efficient generator design using axial type of construction is possible due to their high residual flux density and large coercivity. The circumferential type is suitable for generators with large number of poles and using magnets with low residual flux density.

1.3 Axial Flux Generator

The axial flux PM motor is an attractive alternative to the cylindrical radial flux motor due to its pancake shape [7], compact construction and high power density. Axial flux PM motors are also called disk-type motor.

1.3.1 Geometries

Axial flux PM motors can be designed as double-sided or single-sided machines, with or without armature slots, with internal or external PM rotors and with surface mounted or interior type PMs.

1.3.1.1 Single Sided Machine

Single sided AFPM machines (Fig. 1.2) with stator ferromagnetic cores have a single PM rotor disk opposite to a stator unit consisting of a winding and ferromagnetic core. The stator ferromagnetic cores can be slotted or slotless. The stator winding is always made of flat wound coils. The PMs can be mounted on the surface of the rotor or embedded (buried) in the rotor disc. In the case of a slotless stator the magnets are almost always surface mounted, while in the case of a slotted stator with a small air gap between the

rotor and stator core, the magnets can be either surface mounted on the disc or buried in the rotor disc. Single-sided construction of an axial flux motor is simple, but the torque produced is low. Large axial magnetic forces on bearings are the main drawback of single sided AFPM machines with ferromagnetic stator cores.



Figure 1.2: Single sided AFPM machine

1.3.1.2 Double Sided Machine

In double sided AFPM machines with ideal mechanical and magnetic symmetry, the axial magnetic forces are balanced. In the double-sided motor with internal PM disk rotor (Fig. 1.3a), the armature winding is located on two stator cores. The disk with PMs rotates between two stators. A double sided motor with internal stator (Fig. 1.3b) is more compact than the previous construction with internal PM rotor [8, 9, 10, 11]. The double-sided rotor with PMs is located at two sides of the stator. Disk-type motors with external rotors have a particular advantage in low speed high torque application due to their large radius for torque production. As with single-sided AFPM machines the stator ferromagnetic cores can be slotted or slotless, and the rotor magnets can be surface mounted, embedded or buried. Again, in the case of a slotless stator with a large air gap

between the rotor and stator core the magnets are almost always surface mounted. The stator windings of double sided AFPM machines can be flat wound (slotted or slotless) or toroidally wound (normally slotless).

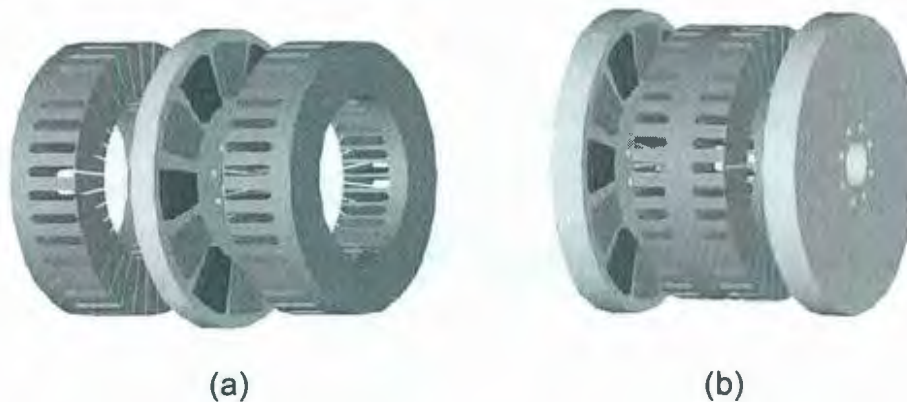


Figure 1.3: Double sided AFPM machine (a) internal rotor (b) internal stator

1.3.1.3 Ironless Double Sided Machine

AFPM machines with coreless stators have the stator winding wound on a non-magnetic and non-conductive supporting structure or mould. The stator core losses, i.e. hysteresis and eddy current losses do not exist. The losses in PMs and rotor solid steel disc are negligible. This type of design offers higher efficiency at zero cogging torque. In order to maintain a reasonable level of flux density in the air gap, a much larger volume of PMs in comparison with laminated stator core AFPM machine is required. The stator winding is placed in the air gap magnetic field generated by the PMs mounted on two opposing rotor discs.

1.3.1.4 Multidisk Machine

There is a limit on the increase of motor torque that can be achieved by enlarging the motor diameter. Factors limiting the single disk design are: (a) axial force taken by bearing, (b) integrity of mechanical joint between the disk and shaft and (c) disk stiffness. A more reasonable solution for large torques is double or triple disk motors (Fig. 1.4). The number of modules depends on the requested shaft power or torque. The disadvantage of this type of multi disk motor is that a large number of bearing equal to double the number of modules are required.



Figure 1.4: Multidisk AFPM machine

1.3.1.5 Rotor Configuration

Depending on the location of the magnets in the rotor, the permanent magnet generator can be classified into three different configurations, namely the surface mounted, interior, and inset type [6, 12, 13].

Interior:

The interior-magnet rotor (Fig. 1.5) has radially magnetized and alternately poled magnets. Because the magnet pole area is smaller than the pole area at the rotor surface, the air gap flux density on open circuit is less than the flux density in the magnet [14]. The magnet is very well protected against centrifugal forces. The interior PM generator has narrow and smooth air gap. The motor torque is contributed by reluctance component due to the difference between direct and quadrature axis reactance as well as the permanent magnet field component. Such a design is recommended for high frequency high speed motors.



Figure 1.5: Interior magnet rotor

Surface mounted:

The surface mounted motor (Fig. 1.6) can have magnets magnetized radially or sometimes circumferentially. The direct and quadrature axis reactance are practically same in surface magnet type. Permanent magnets are not protected against armature fields which cause eddy current loss in permanent magnets (when their conductivity is greater than zero). An external high conductivity non ferromagnetic cylinder is sometimes used. It protects the PMs against the demagnetization action of armature reaction and centrifugal force, provide an asynchronous starting torque, and act as a

damper [7]. The machine with surface magnet is essentially non-salient type. It has a large air gap. The large air gap weakens the armature reaction effect, and therefore the operation is essentially restricted to low speed and constant torque region [6].

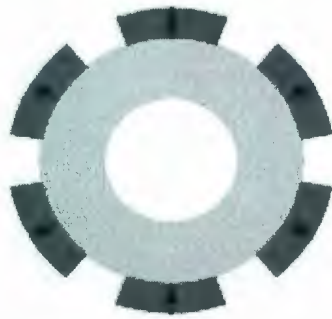


Figure 1.6: Surface mounted magnet rotor

Inset:

In the inset-type motors (Fig. 1.7) PMs are magnetized radially and embedded in shallow slots. The rotor magnetic circuit can be laminated or made of solid steel. A starting cage winding or external non ferromagnetic cylinder is required. The inset PM generator has a small but relatively smooth air gap. The quadrature axis reactance is greater than that in the direct axis.



Figure 1.7: Inset magnet rotor

Buried:

The buried –magnet rotor (Fig. 1.8) has circumferentially magnetized PMs are embedded in deep slots. In this type the air gap magnetic flux density is greater than B_r . The synchronous reactance in quadrature axis is greater than in that direct axis. The application of a non ferromagnetic shaft is essential. With a ferromagnetic shaft, a large portion of useless magnetic flux goes through the shaft [15]. A buried-magnet rotor should be equipped with a non ferromagnetic shaft or a non ferromagnetic sleeve between the ferromagnetic shaft and rotor core should be used.

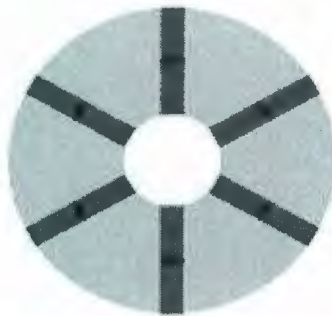


Figure 1.8: Buried magnet rotor

1.3.2 Axial Flux Disk-Type Structure

AFPM disc machines can be constructed in different forms. These machines have N stators and $N+1$ rotors ($N \geq 1$) for external rotor and internal stator surface magnet PM disc motor (TORUS) types and $N+1$ stators and N rotors ($N \geq 1$) for internal rotor and external stator surface magnet PM disc motor (AFIR) types. If N is chosen as 1, the structures have either a single stator sandwiched between two disc rotors (the TORUS topology) or a single rotor sandwiched between two stators (the AFIR topology). The axial flux topologies are shown in Fig. 1.9a-d.

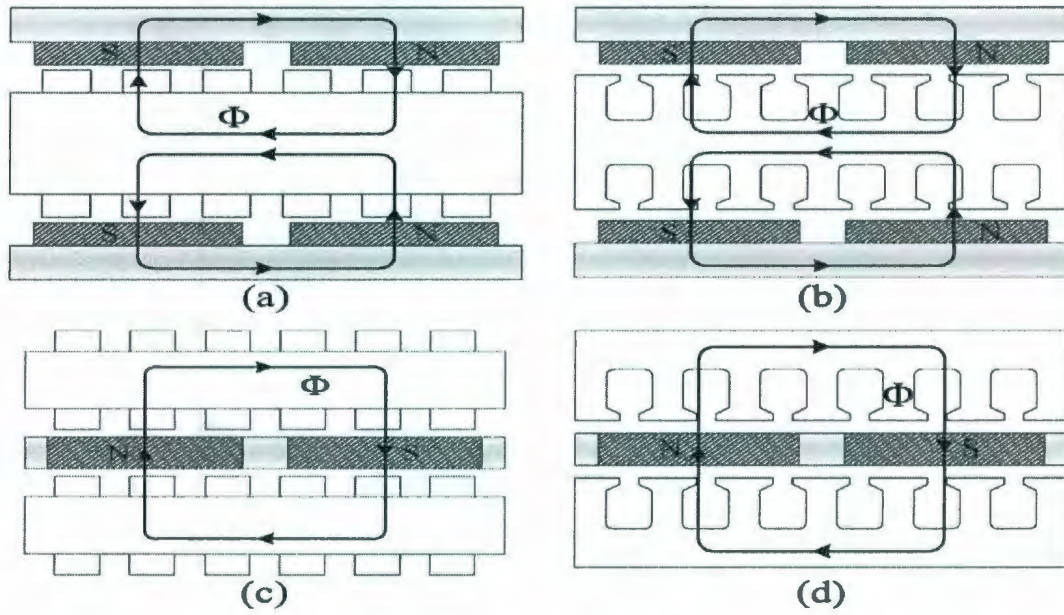


Figure 1.9: AFPM disc-type motor structures: (a) slotless TORUS, (b) slotted TORUS, (c) slotless AFIR, and (d) slotted AFIR machines.

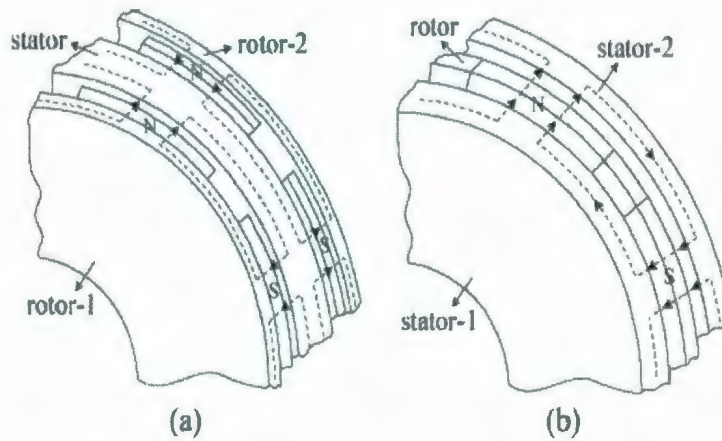


Figure 1.10: Three-dimensional (3-D) flux paths of the (a) TORUS and (b) AFIR type topologies

The basic flux paths of the TORUS and AFIR topologies are shown in Fig. 1.10a-b, respectively. As can be shown in Fig. 1.10a (for the TORUS machines), the N magnets drive flux into the stator core through the air gaps. The flux then travels circumferentially along the stator core, returns across the air gaps, and then enters the rotor core through the opposite polarity of the magnets. In the AFIR-type machines shown in Fig. 1.10b, the magnets with the polarity of N drive flux across the upper air gap into the upper stator core. The flux then travels circumferentially along the upper stator core, returns to the upper air gap, then enters the lower stator core through the S pole of the magnets, and closes its path.

Two different slotted TORUS type machines, namely TORUS NN (North- North) type and TORUS NS (North-South) type, can be derived depending on the direction of the main flux, which are both illustrated in Fig. 1.9a-b. Both machines have a single stator and two surface mounted PM rotor discs. The stator has a slotted structure with tape wound stator iron. Back-to-back connected windings are placed into back-to-back slots in NN type structure while the conventional 3-phase windings are used in each side of the NS type structure. The rotor structures are exactly the same in both machines, which are composed of surface mounted axially magnetized magnets and rotor discs. The differences between the two structures are the magnetization direction of the magnets, existence of the stator core, the flux paths and winding structure.

In order to create the appropriate flux path, the magnets facing each other on each rotor should be N and N poles or S and S poles in TORUS NN type and, N and S or S and N poles in TORUS NS type. Therefore, the direction of armature current must be changed appropriately so as to create torque [16].

1.3.3 Performance Characteristics

The performance of PM axial flux machine highly depends on the torque quality. Torque quality depends not only on torque density (both torque-to-volume and torque-to-weight ratios) but also the pulsating torque.

The torque components are:

- 1) Cogging torque is the pulsating torque component produced by the variation of the air gap permeance or reluctance of the stator teeth and slots above the magnets as the rotor rotates. No stator excitation is involved in cogging torque production.
- 2) Torque ripple is the pulsating torque component generated by the stator MMF and rotor MMF. In surface mounted PM machines, torque ripple is mainly created by the interaction between the MMF caused by the stator windings and the MMF caused by the rotor magnets because there exists no rotor reluctance variation.
- 3) Pulsating torque is the sum of both cogging and torque ripple components.
- 4) Total torque is the sum of average torque and pulsating torque components.

1.3.3.1 Cogging Torque

Cogging is the oscillatory torque caused by the tendency of the rotor to line up with the stator in a particular direction where the permeance of the magnetic circuit “seen” by the magnets is maximized. Cogging torque exists even when there is no stator current. When the motor is running, additional oscillatory torque components can result from the interaction of the magnet with space harmonics of the winding layout and with current

harmonics in the drive current. These additional oscillatory torque components are electromagnetic and are generally referred to as torque ripple, while the term cogging is often reserved for the zero current condition. In a well designed motor the torque ripple and the cogging should both be negligible, but it is possible for the torque ripple to exceed the cogging torque by a large amount if the motor has an inappropriate combination of winding layout, drive current and internal geometry. Existence of these torque mechanisms is a foremost concern in the PM motor design due to the unwanted harmonics added to the motor output torque [17]. These components not only affect the self-starting ability of the motor but also produce noise and mechanical vibrations. Many techniques for cogging torque minimization are documented in the literature for PM machines due to the high demand on PM machines for high performance applications [18, 19, 20, 21, 22, 23].

With a large number of slots/pole the cogging torque is inherently reduced by the fact that the relative permeance variation seen by the magnet is reduced as it successively covers and uncovers the slots one at a time: indeed the permeance variation can be thought of as being concentrated at the edges of the magnet. A small amount of skew is then usually sufficient to eliminate most of the cogging.

Cogging torque can also be compensated electromagnetically by adapting the drive current waveforms to produce an electromagnetic torque ripple component that cancels the cogging [24].

Other methods for reducing cogging include the use of bifurcated teeth or punching holes in the tooth overhangs to modulate the permeance variation [25]. Bifurcated teeth or ‘dummy slots’ have a similar effect to that of doubling the number of

slots: the cogging torque frequency is doubled and the amount of skew required to eliminate the cogging is halved. Also, the permeance variation caused by uncovering a whole tooth, so the magnitude of the cogging torque decreased as well.

1.3.3.2 Pulsating Torque

The AFPM machines can be designed for higher torque-to-weight ratio and higher efficiency and can be considered as a significant advantage over conventional PM machines. Torque quality of AFPMS is an important matter for low-noise smooth-torque PM disc machines and directly related to pulsating torque component. Pulsating torque consists of two components, namely 1) cogging torque and 2) “torque ripple”. Cogging torque arises from the variation of the magnetic permeance of the stator teeth and the slots above the permanent magnets. The presence of cogging torque is a concern in the design of PM machines because it adds unwanted harmonics to the pulsating torque. Torque ripple occurs as a result of fluctuations of the field distribution and the armature magnetomotive force (MMF). At high speeds, torque ripple is usually filtered out by the system inertia [26]. However, at low speeds or gearless-motor direct-drive systems, torque ripple produces noticeable effects that may not be tolerable in smooth-torque and low-noise applications [27, 28, 29, 30].

1.4. Permanent magnet material

1.4.1. History

Permanent magnets has been known science prehistory, first in their naturally- occurring state, known as “lodestones”, in ancient China. PMs have been used in electric machine applications almost from the beginning of the development of these machines as replacements for wound field excitation systems. However, the low energy densities of early manufactured permanents, such as chrome steel and other hard steel magnets, did not permit the use of permanent magnets in any type of machine other than very low power control machines and signal transducers. Modern permanent magnet machines began with the development of Alnico magnets by Bell Laboratories in the 1930’s. The high flux densities and reasonable energy products of Alnico magnets permitted their use in power applications, and permanent magnet motors with ratings up to several horsepower were developed for commercial applications. DC generators and alternators with ratings of many kilowatts were also developed for military and aerospace applications using Alnico magnets. However, the low coercive for this class of PM limited its applications to relatively constant current applications where transient disturbances were not present.

Widespread use of PMs in commercial and aerospace applications were made possible with the advent of ceramic or “hard ferrite” PMs in the 1950’s. Although the flux densities available in this class of PM are much lower than those of the Alnico class, the high coercive force of ferrite PMs made possible the adaptation of PM machines to the conventional machine armature reaction and transient environment. A great many

automotive motors were converted to ferrite PM excitation and, as a result, the PM dc motor is probably the most widely-used dc motor configuration today. The hard ferrite class of PMs generally offers a cost saving over all other types of PMs and is produced in extremely large quantities today for almost all types of PM applications.

The next major evolution affecting PM electric machines came with the advent of commercial rare-earth permanent magnet in the 1960's, and this evolution is ongoing today. The early rare-earth PMs were alloys of cobalt, with samarium as the most common rare earth. Samarium-cobalt PMs offer the high flux density of the Alnico class and an even higher coercive force than the hard ferrite class, resulting in much higher energy densities than any previous class of permanent magnets except for various "exotic" and costly alloy such as platinum-cobalt. Samarium-cobalt, while having excellent technical characteristics, is relatively expensive and uses a large percentage of cobalt, which is a strategic material in several parts of the world today. A more recent development in rare earth PMs is the neodymium-iron-boron (NdFeB) alloy which has PM characteristics comparable or superior to most of the samarium-cobalt alloys and has the potential for much lower cost. It uses no strategic materials and neodymium is one of the most plentiful of the rare earth elements. Experimental NdFeB magnetic materials have exhibited the highest energy density of any known permanent magnet materials. PM machines using NdFeB magnets have the potential for application in most electric machine application today.

1.4.2. PM material

Permanent magnets used in rotating electric machines are of two general classes: ferromagnetic materials and ferrimagnetic materials. Ferrimagnetic permanent magnets, often called hard ferromagnetic materials, are crystalline structures formed from metallic alloys, usually containing one of the three natural magnetic metals, iron, nickel, or cobalt. Ferromagnetic materials, are often called hard ferrites, are oxides of iron and one other metal, usually barium or strontium.

In general, all magnetic materials exhibit varying degrees of permanent magnetism, often called remnance. To place a magnetic material in a state of zero magnetism requires a process known as “de-magnetization”, by means of an externally applied magnetic field. However, hard magnetic materials or permanent magnets are those magnetic materials which retain a much higher level of magnetism than “soft” magnetic materials in the absence of an external magnetic field. This property results from the internal microscopic structure of permanent magnet (PM) materials, which also causes differences in most other physical properties of hard and soft magnetic materials. PM materials generally are hard and somewhat brittle and have lowered tensile and bending strength than soft magnetic materials. Their Curie temperatures and other thermal characteristics also differ from those of soft magnetic materials.

Alnico magnets:

Alnico PM Materials are metallic alloys of aluminum, nickel, cobalt, and iron, and were among the first high energy PMs to be developed. Developed at the Bell Lab and GE in the 1930's, Alnico magnets are still widely used and manufactured throughout the world.

Alnico magnets are still widely used and manufactured throughout the world. Alnico magnets are, generally, characterized by relatively high residual flux density (B_r) and relatively low coercive force, (H_c). The later characteristic is undesirable from the electric machine standpoint. Certain grades of Alnico, such as grade 8HC, have been developed to remedy this weakness, but at the expense of lowered residual density.

Ceramic magnets:

Ceramic magnets are similar to other types of materials commonly referred to as ceramics in physical properties. However, ceramic PMs are properly defined as ferrite oxides of barium or strontium and exhibit the property known as ferrimagnetisms. Ferrites are brittle and have little mechanical strength and should not be used as structural members of a machine.

Ceramic magnets are characterized by relatively low residual flux densities (B_r) and relatively high coercive forces (H_c). Because of the later characteristic, ceramic magnets are able to withstand armature reaction fields without demagnetization and are well suited for electric machine applications. Although ceramic magnets have generally poor mechanical and structural characteristics, they are the lightest in density of the common magnet types. This is often a distinct advantage in machine applications and tends to compensate for the increased pole-face area required due to the low residual flux density. Also, ceramic magnets have the lowest recoil permeability of common magnets, which is stabilizing factor in machine application.

Samarium cobalt:

The first commercially feasible rare earth magnets were developed by K. J. Strnat, and are now widely available from a number of manufacturers throughout the world. Samarium-cobalt magnets gave an “order-of-magnitude leap” in energy product over ceramic magnets and most other types of magnets. Samarium-cobalt magnets have residual flux densities comparable with Alnico and coercive forces three to five times those of ceramic magnets. These magnets also have generally improved physical characteristics as compared to both Alnicos and ceramics. From a technical standpoint, they are ideal for rotating electric machine applications. However, there are major disadvantages for commercial use: very high material and manufacturing cost and the strategic nature of cobalt. Samarium is one of the less plentiful rare earth materials and its processing costs are also high.

NdFeB:

Neodymium-iron-boron (NdFeB) PM materials appear to offer the greatest promise for a PM material with greatly improved characteristics over those of ceramic magnets. This material has been shown in the laboratory to have the highest energy product of any PM material, and the commercial versions of these laboratory samples are available with energy products above those of samarium cobalt. Perhaps more importantly, NdFeB magnets hold the promise of relatively low cost in production quantities. Neodymium is one of the most available of rare earth elements. Although the major deposits are in mainland china, there are large deposits in the US and the other western countries. Processing costs are lower than those of samarium. Also no strategic materials are used in the alloys of this magnet.

NdFeB has the highest coercive force available in commercial magnets and, therefore, is ideally suited for machine applications. Also its residual flux density is relatively high, comparable to the best of the Alnicos.

Its energy product is the highest available today. Limitations of this material include very poor temperature characteristics. The low operating temperature requires the use of a large size for an application required to operate at elevated temperatures and, therefore, many of the reduced size and weight advantages of NdFeB are lost.

The addition of cobalt or some other rare-earth materials to NdFeB is claimed to improve the thermal characteristics of this magnet [31]. This material, which contains a large amount of cobalt, and many require additional weight and size in corrosion protection materials in some application.

1. 5. Aim of this work:

The purpose of this project is to extract few watts electrical power from the sea-floor ocean current. To meet the requirement the study focuses on the design a generator which is suitable for under water application and can produce electricity from the low marine current velocities (usually less than 100rpm).

The gearbox is the moving part used in between the turbine and generator in the conventional drive train. The gearbox adds to the weight, generates noise, demands maintenance and increase losses and reduces reliability. Permanent generators are now widely used for low speed application where the gearbox is eliminated and the generator is directly driven by the turbine.

The aim of this research work is to design a low speed direct driven generator for gearless marine current application. The hypothesis of this work is that the typical generator-gear solution in the marine current power plant can be replaced by a low speed PM synchronous generator.

Chapter 2

2. REVIEW OF RELATED WORK

In this chapter several literatures related to this thesis is presented. Before designing the generator, several works are reviewed. The literature review is presented in three different sections. To choose the generator topology, comparison between different PM generators and different geometries of AFPMG is reviewed. For the first prototype, different cogging torque minimizing techniques are analyzed. Also works related to the ironless stator is studied.

2.1 Comparison of PM generators

Basically, PM generators can be divided into radial-flux and axial-flux machines, according to flux direction in the air gap. Transverse flux machines exist, but do not seem to have gained a foothold in direct drive generation. Many papers have been written to compare different topologies of radial flux and axial flux generators in different aspects.

Sitapati [32], et al. [2000], gives a comparison between the traditional radial field PM brushless machine and different configurations of axial field Pm brushless dc machine. The comparison consist of required copper, steel and magnet weights, copper and iron loss, moment of inertia, torque per unit moment of inertia, power per unit active weight and power per unit active volume for different power levels. According to the outcomes of this paper, the axial field machines have a smaller volume for a given power

rating making the power density very high. For a given magnet material and air gap flux density, the rotor moment of inertia of the radial field tends to be larger than all of the axial field machine in this comparison. The weight of iron required in the radial field motor making the active weight of axial field machines smaller.

Cavagnino [33], et al. [2002], compares the axial-flux versus conventional radial-flux structures for Pm synchronous motors. Two motor topologies are compared in terms of delivered electromagnetic torque and torque density. The comparison is developed for different motor dimensions and the pole number influence. The overall motor volume, the losses per wasting surface and the air gap flux density are kept constant. The presented comparison brings to the conclusion that the considered AFPMs are an attractive solution if the number of pole is high (≥ 10) and the axial length is short (< 0.3).

Silaghi [34], et al. [2005], provides a comparison among PM generators of seven different topologies consisting of both radial-flux and axial-flux machine. In this paper to compare machine topologies, a large number of prototypes is designed and obtain sufficient information to draw the general conclusion. Optimum design is considered for each prototype. It is inferred that axial-flux slotted machines have a smaller volume for a given power rating, making the power density very high. However, it should be mentioned that as the power rating is increases and the outer radius becomes larger, the mechanical dynamic balance must be taken into consideration for axial-flux machine. The two sided axial-flux configuration is superior to the one sided axial-flux configuration. For all of the comparisons, the outer-rotor construction is superior to the inner-rotor construction. The Torus construction is simple and more suitable for low power rating generators.

Different machine topologies have not been compared very much with each other in this literature. However, the comparison shows that the conventional radial flux machine will not be suitable design for a low speed directly driven generator. The axial flux machine is smaller in volume and has a high power density. The axial flux machine is a better choice if the speed is very low i.e. the number of pole is high.

2.2 PM Axial Flux Generator

Many papers have been written on axial-flux PM generators. Performance comparison between different machine topologies is not a straight forward task as many variables exist in electromagnetic, thermal and mechanical aspects. Sitapati [32], et al. [2000], compares one radial field and four axial field topologies for five different output power level. The comparison consists of volume, weight, power loss and inertia. All the machines are designed with surface mounted PM rotors – conventional radial field, axial field single air gap, axial field dual air gap, axial field slotless single air gap, axial field slotless dual air gap. The slotless axial field machines require more magnet material than the slotted one. The slotless machines require a larger diameter due to the additional turns. So the copper loss in the slotless machine is higher than that of slotted one. The single air gap motor has more electromagnetic loss than dual gap axial field machine.

An axial-flux machine with toroidal air-gap winding has been presented by Soerlund [35], et al. [1996]. NdFeB permanent magnets are mounted on two rotor discs on both sides of the stator. A 5kW and a 10kW experimental machine have been built and tested. The machines have 14 poles. Special attention must be paid to the choice of

structural materials. If the casing is too close to the rotating magnets, the leakage flux will induce eddy currents causing extra losses and heating. A 100kW, 90 pole experimental machine is under construction.

Chalmers [36], et al. [1997], have presented an axial-flux slotless machine with a toroidal air-gap winding. More magnets are needed in a slotless machine than a slotted machine, because the total air gap (air gap + winding thickness) is large. A skewed construction of the stator or rotor is unnecessary in this type of a machine. However, eddy-currents are induced in the winding by the main air-gap flux. A 1.5 KW, 24 poles as well as a large 5 KW experimental machine have been built. The machines are use for in small-scale stand-alone generating systems in remote areas.

Marignetti [37], et al. [2005], deals with an axial flux PM synchronous motor for a direct wheel drive. Its main feature is the armature winding of the fractional slots type. The winding is therefore a concentrated non overlapping one allowing a large number of poles to be achieved in a small diameter. The interest towards compact PM generators is partially due to its small aspect ratio and also to its torque density. The structure is of the single stator double rotor type and the output power is 2 KW. The end winding connections are short in comparison with traditional windings. The induced emf waveform is not distorted, due to equivalence to a machine with two slots per pole and per phase.

Chen [38], et al. [2005], presents low speed directly driven axial flux PM wind generator. Through careful design an axial flux Pm generator with slotted soft magnetic composite (SMC) core is built and tested. The advantage of this type of generator is

better performance, reduced size and weight, low part count and low cost. The best result is that highest torque to weight ratio.

Ferreira [39], et al. [2007], presents a double sided axial flux PM low-speed generator with internal rotor and slotted stators. Such a structure gives a good compromise between performance characteristics and feasibility of construction. The rated power of the prototype at 600rpm is 340w with number of pole pair 10. A simple electromagnetic design model, considering the fundamental laws governing this type of machines was used to achieve and implement a prototype. This effort relies on a set of analytical expressions which lack the precision and accuracy that a final analysis deserves.

2.3 Minimization of Cogging Torque

A variety of techniques exist for reducing the cogging torque of conventional radial flux PM machines. Even though some of these techniques can be applied to axial flux machines, manufacturing cost is especially high due to the unique construction of the axial flux machine stator. Consequently, new low cost techniques are desirable for use with axial flux PM machines.

Muljadi [40], et al. [2002], investigate three design options to minimize cogging torque- uniformity of air gap, pole width and skewing. FEA is used to quantify the cogging torque in the design process. The outcomes include

- a) the cogging torque can be minimized creating a non uniform air gap
- b) there is a minimum cogging torque as the pole arc to pole pitch ratio is varied
- c) a perfect skew can nearly eliminate cogging torque

Aydin [41], et al. [2003], introduces a new cogging torque minimization technique for axial flux multiple rotor surface magnet PM motors. A 3kW, 8-pole axial flux surface magnet disc type machine with double-rotor-single-stator is designed and optimized in order to apply the proposed new method- alternating magnet pole arcs. The analysis has been carried out using 3D FEA. The minimized cogging torque is compared with several existing actual machine data. The analyses show that peak cogging torque components can be reduced greatly with careful and precise calculation of magnet pole-arcs in multiple-rotor machines. Besides the simplicity and cost-effective features of this technique, the results show that the new technique effectively reduces the cogging torque component without any sacrifice on the peak torque and pulsating torque components.

Dosiek [42], et al. [2006], examines two methods of reducing cogging torque in permanent magnet machines: magnet shifting and optimizing the magnet pole-arc. The methods were applied to existing machine designs and the performance calculated using finite element analysis (FEA). Prototypes of the machine designs were constructed and experimental results obtained. It is shown that the FEA predicted the cogging torque to be nearly eliminated by this method but in the prototype there was some residual cogging due to manufacturing difficulties. In both cases, the back EMF was improved by reducing harmonics while preserving the magnitude.

2.4 Ironless Stator Axial Flux PM Machine

Ironless motor do not produce any torque pulsation at zero current state and can reach very high efficiency impossible for standard motors with ferromagnetic cores. Elimination of core loss is extremely important for high speed motors operating at high

frequencies. Another advantage is very small mass of the ironless motor and consequently high power density and torque density. The drawbacks include mechanical integrity problems, high axial forces between PMs on the opposite disks, heat transfer from the stator winding and its low inductance. Small ironless motors may have printed circuit stator winding or film coil windings. The film coil stator winding has many coil layers while the printed circuit winding has up to four coil layers.

Lombard [43], et al (1998), Presents the analysis, design and performance of an AFPM machine with an ironless stator. A machine model that uses both lumped magnetic circuit and finite element method results is used with a multi-variable optimization algorithm to obtain the optimum machine dimension. A prototype machine is constructed and evaluated. Measured results of the armature reaction effect in the large air gap are given and discussed. The prototype machine displayed the expected characteristics of low noise, zero cogging torque and reduced copper losses for a certain power level at the expense of a large magnet volume.

Jang [44], et al (2002), introduces the design and development of an axial-gap spindle motor using printed circuit board (PCB) winding and dual air gaps, which has the mechanical rigidity, high efficiency and zero cogging torque. Superior characteristics of the developed motor can be effectively used for various applications. The paper shows the prototyped motor consumes less power than the radial-gap motor. The copper loss is very small, and both motors have almost the same copper loss under no load condition. But the prototyped motor has much less rotational loss and the difference of rotational loss is getting bigger as the speed increases.

Tsai [45], et al (2006), presents a miniature axial-flux spindle motor with a rhomboidal printed circuit board (PCB) winding. The flexible PCB winding represents an ultra thin electromagnetic exciting source to reduce the end-winding length and minimize the copper loss. The design process also incorporates finite element analysis for further performance evaluation and refinement. The proposed motor is prototyped, and excellent agreement is found between simulation and measurement. The result illustrates that the base-plate is thin enough to suppress noticeable and excessive base-plate eddy current which would lead to a reduction in open-circuit voltage and additional losses.

Reed [46], et al (2008), presents an AFPMA with PCB stator. An AFPMA using this new stator is build, test and compare the results, specifically output power, to alternators of similar size using traditional wound stator. The PCB stators did simplify the design and assembly process of building an AFPMA. The stator has four coils per phase with 36 turns per coil printed on four layer circuit board. The three phases were balanced and the maximum recorded output power was 133 watts at 593RPM. Alternators of similar size produced anywhere from 100 watts to 450 watts at 600 RPM.

2.5 Summary

Several literatures is reviewed and presented in this chapter. In the first section of this chapter, papers related to comparison of different PM generators are studied. From the comparison it is clear that the Axial Flux PM generator is suitable for this thesis because of its high power density and with a smaller size a large number of pole arrangement is possible. The axial flux generator can be of single sided or double sided internal rotor or double sided internal stator type. The single sided has the drawback of a large

uncompensated attractive force between the rotor and the stator. The double sided internal rotor is simple in manufacturing process and less copper loss. The double sided internal stator required less magnetic material in comparison to the internal stator type geometry. The cored axial flux design has better constant where as the ironless axial-gap structure has no iron loss and no need to concern about the cogging torque reduction.

From the above conclusion of the literature review, two prototype- one is double sided internal stator cored type AFPMG and the second one is one is double sided internal stator ironless type, is designed and developed which is presented in the following chapters.

Chapter 3

3. FIRST PROTOTYPE

The design of the first prototype is described in this chapter. First, the background of the design and the hypothesis to minimize the cogging torque is presented briefly. The definition of cogging torque is described in the first chapter (1.3.3.1). Different techniques to minimize the cogging torque which already have been applied in different works is reviewed and presented in chapter two (2.3). The design of the prototyped generator and the techniques applied to minimize the cogging torque is depict later on. The experimental results are presented at the end of this chapter.

3.1. Background

The purpose of this study is to design a generator for gearless marine current turbine. The gearless generator system will reduce the drive line components, thus also reduce the drive line weight. The study focuses on the design of multipole axial flux PM generator. The AFPMG has favorable characteristics concerning efficiency and specific torque compared to conventional designs. For this reason it is especially suited for direct drive application. The AFPMG is also an attractive choice due to its pancake shape [7], compact construction and high power density.

Flux in an axial flux machine flows axial to the direction of rotation. The AFPM machine is basically equivalent to the conventional radial flux surface mount permanent magnet machine geometry. Therefore, they suffer from the well-known low-inductance problem. However, this problem can be substantially mitigated by the high torque density

and good efficiency [47]. The AFMs are an attractive solution if the number of pole is high (≥ 10) and the axial length is short ($\lambda < 0.3$, where, $\lambda = L/D_e$; L = active axial length of stator core in m and D_e = external motor diameter in m) [33].

The axial flux PMG can be of single sided or double sided internal rotor or double sided internal stator type. The double sided are used in order to get balanced axial forces and to increase the total air gap surface. The single sided has the drawback of a large uncompensated attractive force between the rotor and the stator. The double sided internal rotor is simple in manufacturing process and less copper loss.

The stator of the double sided internal stator type can be cored or ironless type. The cored axial flux design has better constant power range compared to the coreless design. The cored stator can be slotted or slotless. The slotless axial field machines require more magnet material than the slotted machine. Also the copper loss in the slotless dual gap machines is higher than the slotted dual gap AFPMG. Slotted stators increase remarkably the amplitude of the air gap flux density. Slotting may evoke undesired torque pulsation but in slotted stators the mutual and leakage inductances are increased compared to the slotless stator which is advantageous.

3.2. Design Consideration

Several features should be taken into account when designing a low speed generator. The characteristics of the machine should be sufficient, for example, the efficiency high and torque ripple low. Furthermore, the dimensions of the machine should not be too large, the weight and the cost should not be too high and the manufacturing process should be simple.

Due to elimination of gears, the machine needs to produce the total torque directly into the wheel shaft. Hence, the size and the weight of the machine tend to grow. Therefore, major challenge in a gearless system is to keep the size and the weight of the machine low for direct in-wheel mounting.

The AFPM machine suffers from low-inductance problem. High torque density and good efficiency can mitigate the problem. The gain in density can significantly exceed if high energy magnets are used. The high torque density in AFPM machine is best achieved by designing the machine with large machine diameter and high machine number of poles. So there should be a trade off between the size, power and weight of the machine.

For the generator with cored stator, the core loss is another concern for designing generator. The core loss contains the hysteresis and eddy current loss. The hysteresis loss is related to the frequency. At higher frequency the loss is high. The eddy current loss is the resistive loss in the core, so it is related to the material properties. So in designing cored stator, the material properties such as resistance and loss at designed frequency of the core should be analyzed.

Existence of the cogging torque is the fore most concern in the PM machine design due to the unwanted harmonics added to the motor output torque. These components not only affect the self starting ability of the machine but also procedure noise and mechanical vibrations. For the low speed generator it is the most important designing consideration as it increases the required starting torque.

3.3. Design topologies for minimizing cogging torque

Torque quality is a very decisive issue for direct- drive permanent magnet generator. There exist two undesired pulsating torque components in PM machines which affect the machine performance, one of which is ripple torque arising from harmonic content of the machine voltage and current waveforms and the other is cogging torque caused by the attraction between the rotor magnetic field and angular variations of the stator reluctance. By definition, no excitation is involved in cogging torque production. Existence of these torque mechanisms is the major challenge in designing PM machine due to the unwanted harmonics added to the motor output torque. These components not only affect the self-starting ability of the machine but also produce noise and mechanical vibrations.

There are many techniques for cogging torque minimization [48-53] including magnet pole shape, skewing stator tooth or rotor magnets, stator slot design, dummy slots on the stator tooth, varying the radial shoe depth and graded air gaps. Most of the techniques mentioned can be applied to axial flux machines. However, the high manufacturing cost of the axial flux machines will be even higher when these techniques are applied [54]. For instance, skewing stator slots by one slot pitch or introducing dummy slots will not only boost the manufacturing cost of the axial flux machine stator but complicate the manufacturing process as well. The overall cogging torque of an axial flux permanent magnet (AFPM) machine consists of several portions each of which is produced in one air gap. The overall cogging torque is reduced by two general approaches: Reducing the amplitude of each portion, similar to what conventional methods accomplish, and shifting the relative phase of the different components so that

they can compensate each other. Consequently, the overall cogging torque will be much reduced at minimal incremental cost.

The following design techniques are applied in our design to minimize the cogging torque. The following design technique is a combination of methods that utilize the aforementioned cogging torque reduction theory.

3.3.1 The TORUS configuration

AFPM disc machines can be constructed in different forms - TORUS types and AFIR types as described in chapter 1.3.2. The stator of TORUS or AFIR topology can be slotted or non-slotted type. Disk-type motors with external rotors have a particular advantage in low speed applications, due to their large radius.

Two different slotted TORUS type machines, namely TORUS NN (North- North) type and TORUS NS (North-South) type, can be derived. The flux direction of both NN and NS TORUS machine is shown in Fig. 3.1b-c. Both machines have a single stator and two surface mounted PM rotor discs.

In order to create the appropriate flux path, the magnets facing each other on each rotor should be N and N poles or S and S poles in TORUS NN type and, N and S or S and N poles in TORUS NS type. Therefore, the direction of armature current must be changed appropriately so as to create torque [55]. Since the windings in the radial direction are used for torque production, the end windings of the NN type machine are much shorter than that of NS type machine. In other words, the winding structure used in the NS type machine results in a longer end winding which implies a bigger outer

diameter, high copper loss, reduced efficiency and power density compared to its NN counterpart. In our design TORUS NN type is chosen for this advantage.

In case of TORUS NN type motor the two rotors are only mechanically coupled not magnetically. So the alternating pole arc and magnetic shift is possible.

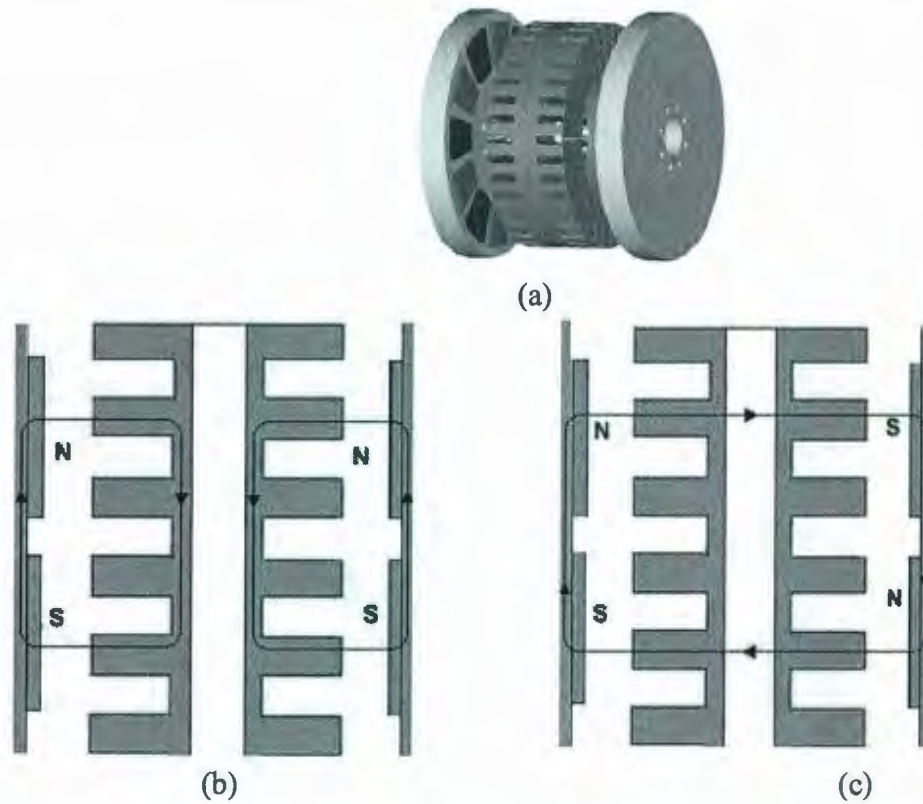


Figure 3.1: Axial flux permanent magnet generator: (a) TORUS Topology (b) NN type
(c) NS type

3.3.2 Alternative pole arc

It is a well-established fact that the magnet pole arc can have a large effect on the magnitude of the cogging torque [56]. By varying the magnet pole-arc (Fig. 3.2) the phase of the cogging torque is shifted [48]. The consequent magnets in each rotor are designed with two different magnet pole-arc ratios: α_m and α_c . The two magnet pole-arc

ratios of the next rotor are same as the previous ones, but in the reversed order, i.e. α_c and α_m , so that the cogging torque produced in each air gap has a phase shift relative to that produced in the consequent. Therefore, the overall cogging torque in any two consequent air gaps could be reduced. The amplitude of each portion can be reduced as well by optimizing the two arcs. In other words, the objective of this technique is to vary the cogging torque phase angle by alternatively using two magnet pole arcs and simultaneously to reduce the amplitude of each portion so that the superposition of the cogging torque variation of all air gap adds up to a very small value.

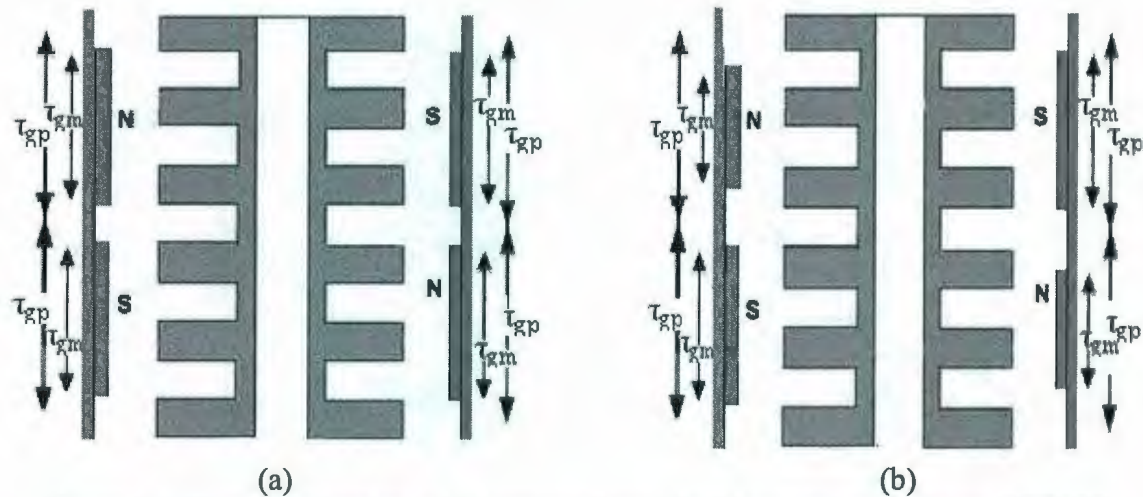


Figure 3.2: Two pole section of (a) conventional double rotor single stator TORUS machine with the same magnet pole-arc and (b) TORUS machine with alternating pole arcs

3.3.3 Magnet shifting

In traditional machines, the cogging torque contributions from each magnet are in phase and thus add to produce the full cogging effect. To avoid this additive effect, the magnets can be shifted relative to each other to place each magnet's cogging torque out of phase

with the others. Shifting the relative phase of the different components can compensate each other [56]. Fig. 3.3 shows only 6 poles, in our design the number of pole is 100.

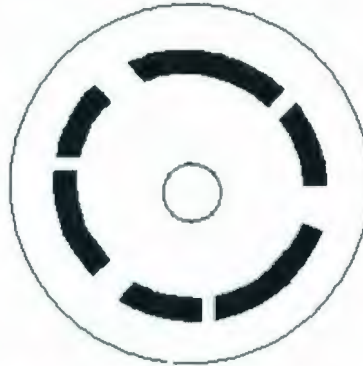


Figure 3.3: Simplified Cross section of a rotor with shifted magnets.

3.3.4 Fractional number of slots per pole

By using a fractional number of slots per pole, each magnet see a fractional number of slots and therefore the cogging torque contribution from the magnets are out of phase with each other, thus reduces the overall cogging torque. The slot per pole combination is an important factor to determine the amplitude and the frequency of the cogging torque [56]

3.4. Design

The final design of the axial flux PMG for under water application is shown in Fig. 3.4. The two rotors are shifted in the TORUS NN topology where two different pole arc ratios are used. The two rotors are mechanically coupled using the shaft, hub and the bearing. The stator is fixed with the frame of the generator with 6 brackets.

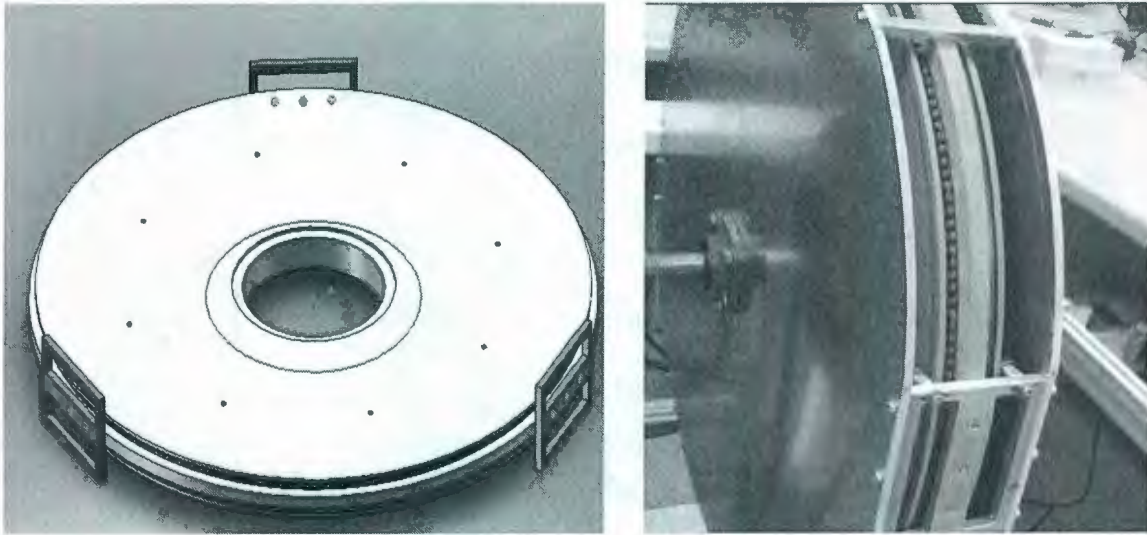


Figure 3.4: The first prototyped generator

3.4.1 Permanent –magnet material

The PM chosen for the design is NdFeB. NdFeB has PM characteristics comparable or superior to most of the samarium-cobalt alloys and has the potential for much lower cost. It uses no strategic materials and neodymium is one of the most plentiful of the rare earth elements. NdFeB has the highest coercive force available in commercial magnets and, therefore, is ideally suited for machine applications. Also its residual flux density is relatively high, comparable to the best of the Alnicos. Its energy product is the highest available today. Limitations of this material include very poor temperature characteristics.

The chosen magnets are of NdFeB of N42 grade which means that the maximum energy product (BH_{max}) is around 42 MGOe. The residual flux density (B_{rmax}) is 13.2 KGs and coercive force (H_c) is greater than 11 KOe and the inductive coercive force (H_{ci}) is greater than 12 KOe. Curie temperature is 310°C .

TABLE 3.1 Magnet properties

Properties	Values
Tolerances	$\pm 0.002'' \times \pm 0.002'' \times \pm 0.002''$
Material	NdFeB, Grade N42
Plating/Coating	Ni-Cu-Ni (Nickel)
Magnetization Direction	Thru Thickness
Weight	0.271 oz. (7.68 g)
Pull Force	13.15 lbs
Surface Field	4871 Gauss
Max Operating Temp	176°F (80°C)
Brmax	13,200 Gauss
BHmax	42 MGOe
Coercive Force(Hc)	>11.0 KOe
Intrinsic Coercive Force (Hci)	>12 KOe

3.4.2 Number of Pole

Where a dc output is required, as in present case, the a. c. output is rectified so no particular frequency of machine emf is demanded. At low speeds in direct network applications lots of poles are needed. The magnetizing inductance L_m of a rotational field machine is inversely proportional to the square of the pole pair number p . In synchronous machines a low synchronous inductance, however, is a benefit because the peak torque of the machine [55] is inversely proportional to the synchronous inductance L_s which consists of the magnetizing inductance and the stator leakage L_σ as:

$$L_m \approx \frac{1}{p^2} \quad (3.1)$$

$$T_{\max} \approx \frac{1}{L_s} \quad (3.2)$$

$$L_s = L_m + L_\sigma \quad (3.3)$$

The number of poles is calculated from the fundamental equation:

$$n = \frac{120 \cdot f}{p} \quad (3.4)$$

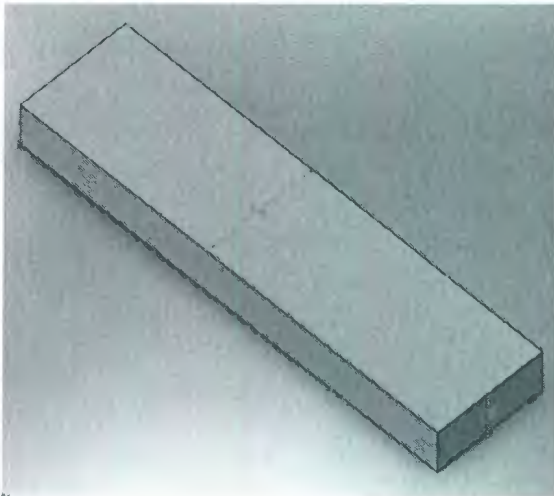
Where n is the mechanical rpm, f is the electrical frequency and p is the number of pole. Mechanical rpm is available from the turbine is only 72. As the electrical frequency is not concern for this design, so chosen 60 Hz. According to the equation, so the number of pole is 100.

3.4.3 Rotor

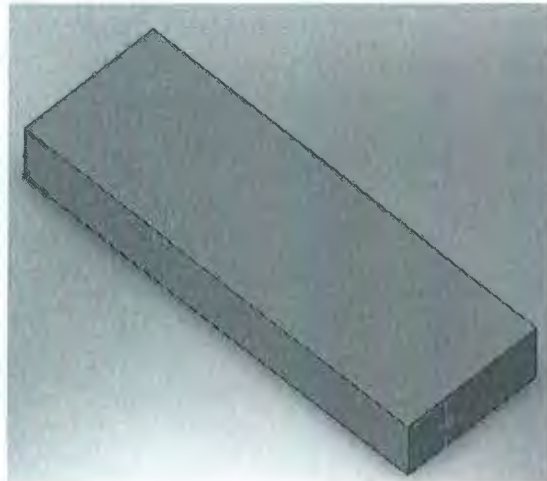
The permanent magnets in the external rotor of a double sided structure are located on the surface of the rotor disk. Thereby, the main flux may flow axially through the rotor disk or flow circumferentially along the rotor disk. With the permanent magnets located at the surface of the rotor disk, it is not necessary a ferromagnetic rotor core and the axial length are substantially reduced, which consequently improves the power density of the machine [10]. The flux path associated with this machine topology is shown in Fig. 1(b). The flux travels axially in the rotor structure and completes its path by returning circumferentially around the stators cores. The rotor of the machine is made by the RENSHAPE (www.mfcomposites.com) material to achieve a minimum generator mass. As the rotor base material is not made by magnetic material, so to have a continuous magnetic path a ring of steel material is placed by making a groove.

TABLE 3.2 RENSHAPE material properties

Properties	Values
Hardness Shore D	54
Density (g/cc)	0.55
Density (lbs/ft.3)	34
Tensile Strength (psi)	1,300
Compressive Strength (psi)	1,400
Compressive Modulus Elasticity (psi)	105,000
Flexural Strength (psi)	2,300
Flexural Modulus (psi)	106,000
Glass Transition Temp (°F)	203
Coefficient Thermal Expansion (in/in/°F)	34.4×10^{-6}
Color	Red. Brown

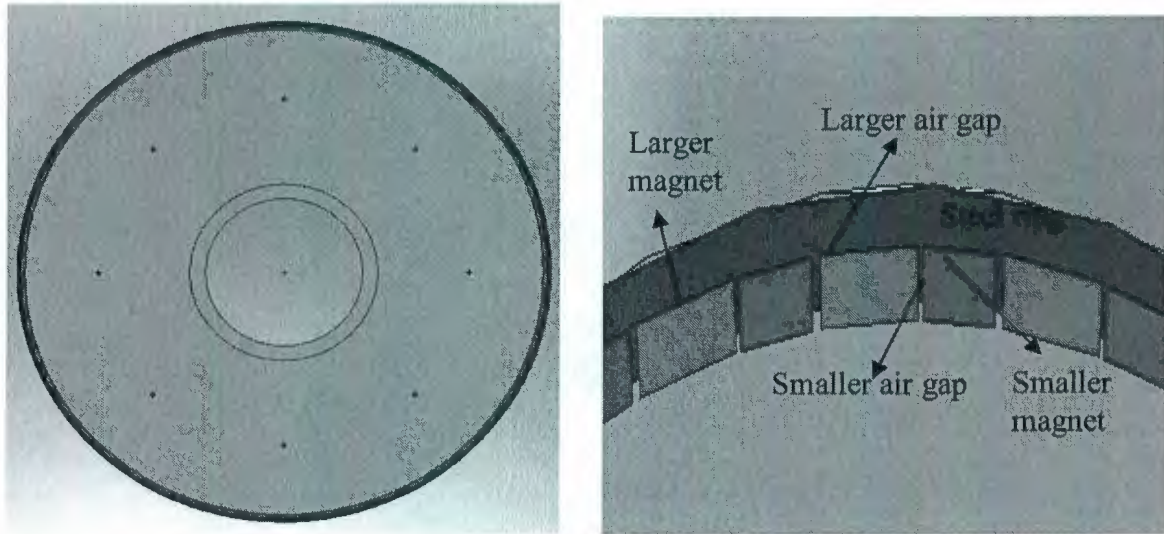


(a)



(b)

Figure 3.5: Permanent magnet (a) Larger (b) Smaller



(a) (b)
Figure 3.6: The rotor (a) full view with magnets (b) sectional view

3.4.4 Stator

For the TORUS configuration, the stator can be slotted or non-slotted type. Slotted stators increase remarkably the amplitude of the air gap flux density due to the shorter air gap and consequently this reduces the required amount of permanent magnets, which yields savings in the generator price [57]. It should be noted also that in slotted stators, the leakage and mutual inductances are increased compared to the slotless stators, which is advantageous for the torque production. The stator slots are built with ferrite E-cores. Ferrite is the component which gives steel and cast iron magnetic properties, and is the classic example of a ferromagnetic material. The main advantage of the ferrite E-core is that at low frequency the core loss is very low.

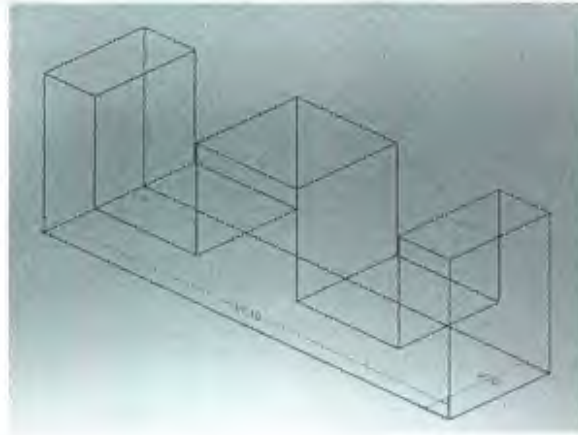
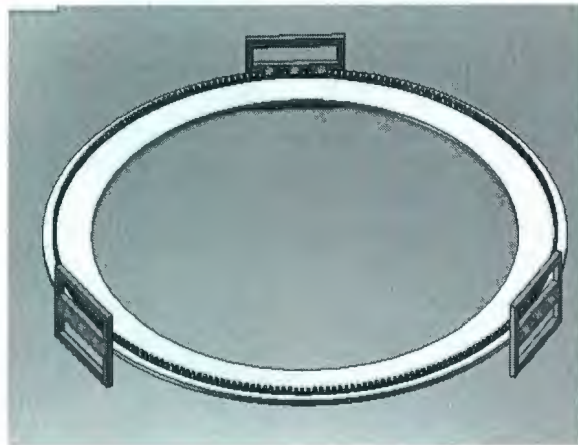


Figure 3.7: E-Core with dimensions



(a)



(b)



(c)

Figure 3.8: The stator (a) solid works design (b) stator with E-core (c) Stator with winding

3.4.5 Stator Winding

In the stator core, there are 300 slots in each side. The number of turns per coil is only 4. For the stator winding AWG 20 is used. The properties of the wire are shown in Table 3.3. The winding is done by hand though it is tedious and complicated. After winding the core epoxy is used.

TABLE 3.3 Properties of AWG 20

Properties	Values
Conductor Diameter (inch)	0.032
Conductor Diameter (mm)	0.8128
Ohms per 1000 ft.	10.15
Ohms per km	33.292
Maximum amps for chassis wiring	11
Maximum amps for power transmission	1.5
Maximum frequency for 100% skin depth for solid conductor copper	27 kHz

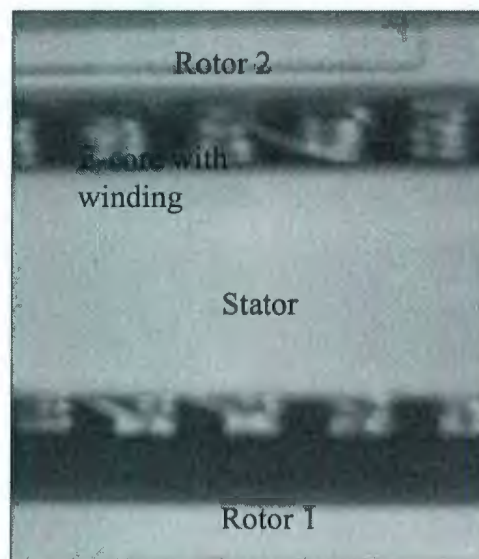


Figure 3.9: A sectional view of prototyped generator

TABLE 3.4: Generator design parameters

Outer radius, r_o [mm]	380
Magnet spacing, τ_f [mm]	2.5 & 1.5
Number of magnets, N_m	100
Number of coils, N_s	4
Number of phases, N_{ph}	1
Magnet thickness, l_m [mm]	1.55
Air gap, δ [mm]	1
Dimension of larger magnet (inch)	1.0×0.25×0.0625
Dimension of larger magnet (inch)	0.75×0.25×0.0625

3.5 Calculated Result

The generator is designed to generate about 12V at a speed of 72rpm. The generator has 100 poles on each of the rotor discs which results in an electrical frequency of 60 Hz at rated speed from equation 3.4.

Induced voltage is calculated by-

$$E_{rms} = \frac{E_{max}}{\sqrt{2}} = \frac{2\pi}{\sqrt{2}} \times N \times f \times \phi_{max} \times \frac{N_s}{N_{ph}} \quad (3.5)$$

Where,

N - Number of turn per coil

N_s - Number of slots

N_{ph} - number of phases

f - electric frequency

Φ_{max} - peak value of the fundamental flux

Φ_{\max} is calculated from-

$$\phi_{\max} = A_{\text{magn}} \cdot B_{\max} \quad (3.6)$$

Where,

A_{magn} - magnet area

B_{\max} - maximum air gap flux density

Air gap flux density is calculated by-

$$B_{\max} = B_r \cdot \frac{l_m}{(l_m + \delta)} \quad (3.7)$$

Where,

B_r - remnant flux density of the magnet

l_m - magnet length

δ - Air gap length between the two rotors

The length of the magnet in the direction of flux is 0.062 inch or 1.6 mm. The air gap length is the sum of the mechanical clearance between the magnet and the E-core and the height of the E-core. The air gap between the rotor and the stator is 1.0 mm on both sides. The height of the stator E-core is 5.7mm. So the total air gap length is about 6.7 mm. So from equation 3.7, the maximum air gap flux density is 0.25T. This would give a rather optimistic value of the air gap flux density. To get a more realistic value an empirical correction factor of 0.75 is used. After correcting the value with the correction factor a maximum air gap flux density of 0.19 T is given.

The remnant flux density of the magnet is 13 Kilo Gauss (KG) or 1.3 Tesla (T). The area of the magnet is (1.0 inch \times 0.25 inch) 0.25 inch² or 1.6e-4 m² for large magnet and (0.75 inch \times 0.25 inch) 0.19 inch² or 1.21e-4 m². Using the magnet area and the

maximum air gap flux density in equation 3.6 the maximum fundamental flux from each magnet is found 0.27×10^{-4} Weber (Wb). From the equation 3.5, the number of turns can be calculated to produce required voltage. For this machine 5.5 turns will induce 12 volt. As the number of turns is a fraction, so the number of turns will be the nearest integer number. So the number of turns can be 6 or 5. The wire size calculated was AWG 18. But it is not possible to wind 6 or 5 turns of this wire in the E-core as the height of the E-core is small. So there was a need to compromise between the wire size, number of turns and the wire size. At last 4 turns with the wire AWG 20 is decided. With 4 turns the induced voltage is 8.5 volt.

The total length of the wire is about 200 ft or 60 m. The resistance of the wire is 10.15 ohm per 1000 ft. So the total resistance of the coil is 2.03 ohm. The coil of both sides is connected in series. So the 300 coils (150 coils in each side) are connected in series.

3.6 Test Result

The designed generator is build and tested in Memorial University of Newfoundland. The generator is tested to find out it's the mechanical and electrical properties.

3.6.1 Mechanical parameter test

For a generator the main mechanical properties are the inertia and the friction of the generator. The inertia of the rotor can be calculated easily from the equation 3.8. As the rotor is a solid disk, the equation for the inertia is

$$J = \frac{mr^2}{2} \quad (3.8)$$

Where

J = Inertia of a solid disk

m= mass of the disk

r= radius of the disk

As the radius, r of the rotor is known 39cm and the density of the material is 0.55g/cc.

The volume of the rotor is

$$volume = \frac{4}{3} \pi r^2 h \quad (3.9)$$

Where h is the thickness of the rotor disk. So the inertia mass can be calculated from the volume and so also the inertia. The total inertia is the sum of the inertia for the two rotor disk and the shaft. So the total inertia found is 0.96 kg-m².

The generator friction can not be measured as 12 extra bearing is used to make the generator mechanically stable. Because of the bearing the friction of the generator is too high. As the RENSHAPE material is flexible and the attraction for of the magnet is very high, so to maintain the small equal air gap between the rotor and the stator 12 extra bearing is used.

The initial torque required to move rotate the rotor is measured using weights. The test setup is shown in Fig. 3.10. The weight required to start the rotor is 3.77Kg. Care should be needed for this test as the weight should be in 90 degree with the radius otherwise the angle should be in account. So the initial torque is 14.5 N-m

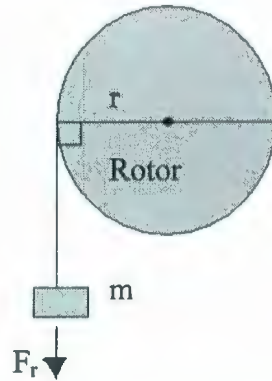


Figure 3.10: Initial torque measurement

3.6.2 Electrical parameter test

To find the electrical parameters of the generator, the generator is tested in the lab. The test setup is shown in Fig. 3.11. The test setup contains the generator coupled to a prime-mover. The developed voltage and generating current is recorded through oscilloscope and multimeter for different load (0-20 ohm) and at different frequency (20Hz, 25Hz, 30Hz, 35Hz, 40Hz, 55Hz, 60Hz, and 70Hz).



Figure 3.11: Test setup for first prototype

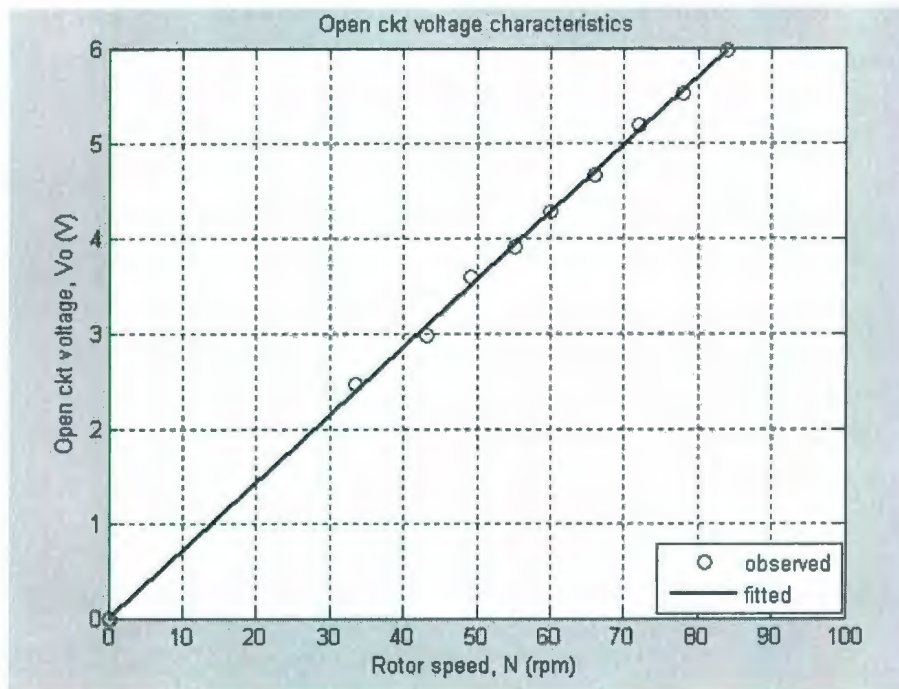


Figure 3.12: Open circuit characteristic of first prototype

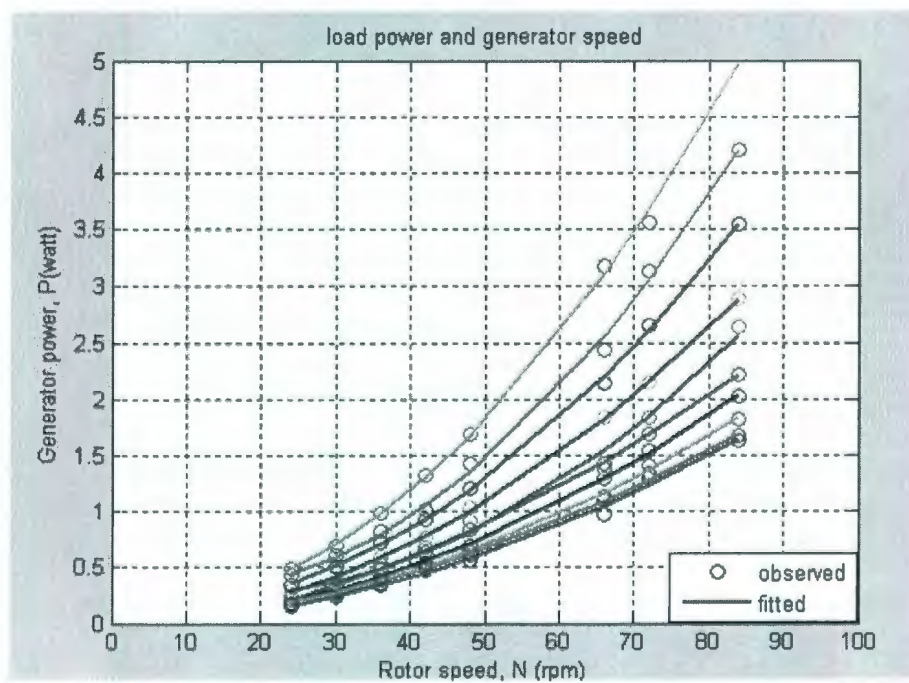


Figure 3.13: Output characteristic of first prototype

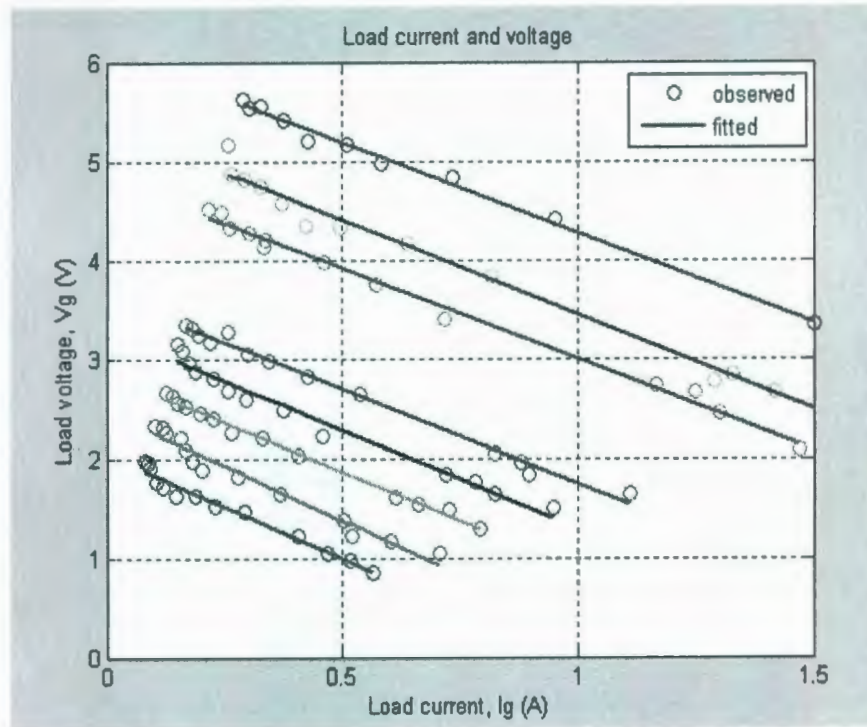


Figure 3.14 load current and voltage of first prototype

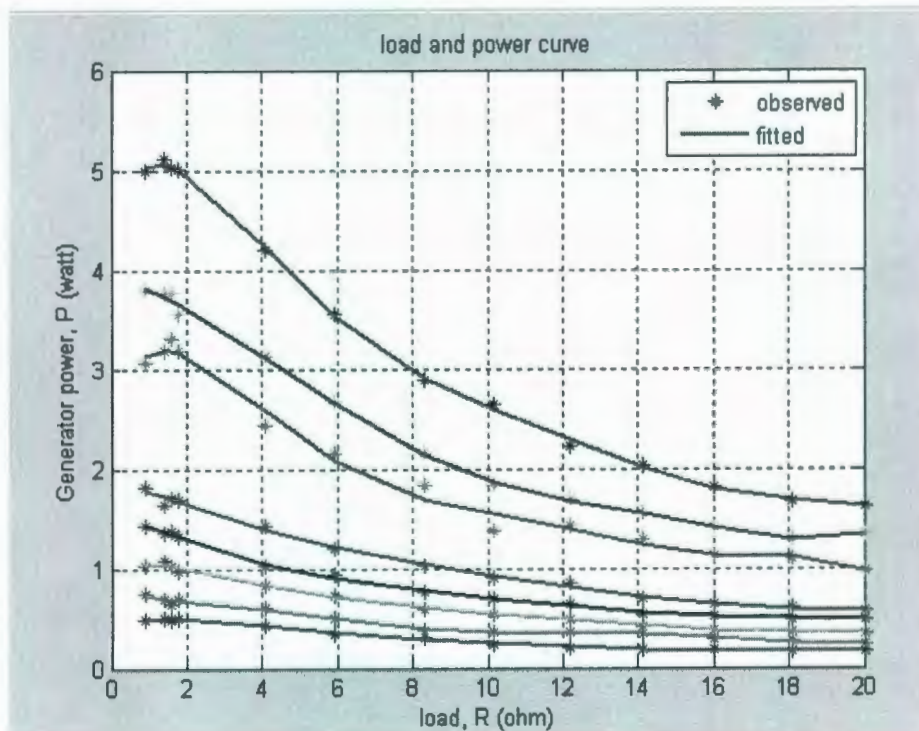
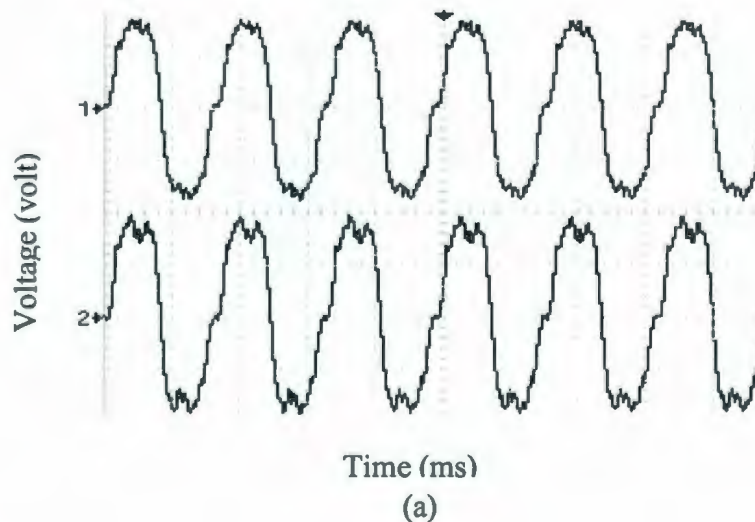


Figure 3.15 Power curve of first prototype

The open circuit test was made under various rotational speeds from 33 to 86 rpm. Fig. 3.12 shows the output open circuit voltage at different operating speed. In the graph the observed data and data fit the polynomial is shown. The test result shows that the output voltage is linearly proportional to the rotating speed.

As the load condition has a significant influence on the output performance of a generator, a resistive load is reasonably used in the experiment. Fig 3.13- fig. 3.15 is the load characteristic of the generator. Fig. 3.13 shows the variation of power output with rotational speed at different load. The variation of induced voltage and current flow at different frequency and load is shown in Fig. 3.14. Here each graph is for a particular frequency with a variation of load. From the curve it is clear that the inductance of the generator is very low which agree with the measured inductance. Fig. 3.15 is the power curve from where the maximum power point can be identified. From the curve, the maximum power is occurred just below 2 ohm. The measured value of the internal resistance of the generator is 1.8 ohm. So the maximum power will be occur at 1.8 ohm. So the graph has the satisfactory agreement with the measured resistance value.



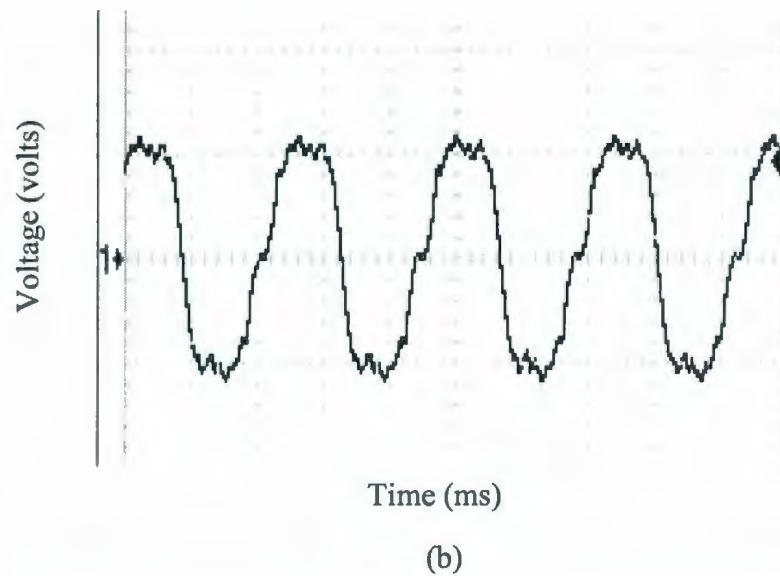


Figure 3.16: The wave form of the first prototyped generator (a) individual wave form of the both side of the stator (b) the resultant waveform of the generator after adding two stators in series (both are taken at 60HZ)

From the Fig. 3.16a, the two wave form for the two stators is exactly in phase. So they can be connected in series to have a larger voltage output. The resultant waveform of the generator after the series connection of the two stators is shown in Fig. 3.16b.

3.7 Circuital model

PMSM are multiphase Synchronous Machines where the magnetic field and rotor rotate in synchronism. However, its operational characteristics are more akin to DC machines. Instead of running only at a synchronous speed, it operates in variable speed variable frequency mode. Also, the torque-speed characteristics are similar to DC machines [58].

In [59], a circuital modeling is approached through classical AC machine theories and a simplified DC machine analogy is established based on the observations. Details and model parameters of a PMSM generator can be found through Finite Element

Modeling and subsequent investigation of design features. Extracting such model parameters and implementing them in computational simulation tools is very laborious.

In this work the circuitual model depicts in [59] is used as shown in Fig. 3.17.

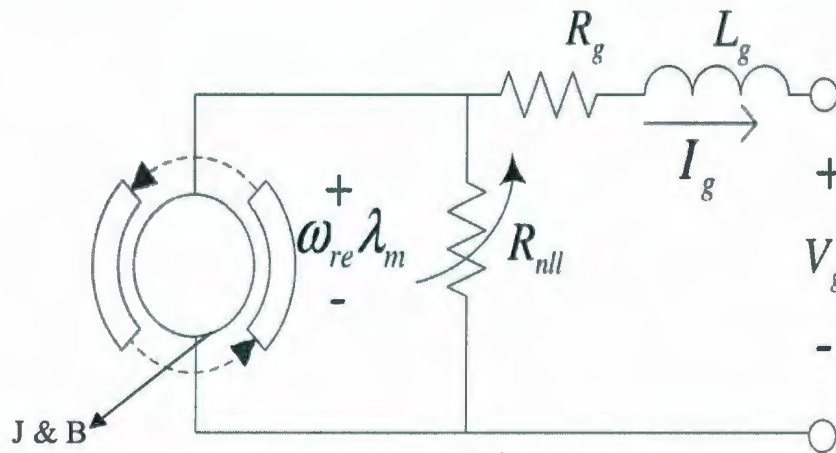


Figure 3.17: Simplified circuitual model of Generator

The test result can reveal inherent characteristic of the machine. The machine constant/ flux linkage λ_m , electrical angular velocity ω_{re} , resistance R_g and synchronous inductance L_g can be found from the test results. The resistance and the inductance is measured using RLC meter, $R_g = 1.8$ ohm and $L_g = 216.7$ μ H. The machine constant λ_m can be determined from the open circuit test. The slope of the linear open circuit voltage characteristic curve yields the parameter λ_m . So from the curve $\lambda_m = 0.071$. The R_{null} is found using the curve fitting approach where R_{null} is found $0.003f^2 + 0.0116f - 0.1458$.

TABLE 3.5: Generator parameters

Internal resistance, R_g , [ohm]	1.8
Internal inductance, L_g [μ H]	216.7
Machine constant, λ_m	0.071
No load loss. R_{null} [ohm]	$0.003f^2 + 0.0116f - 0.1458$
Inertia, J_m [Kg-m ²]	0.96
Initial torque, T_o [N-m]	14.5
Open Circuit voltage at 72 rpm [volt]	5.18
Load for maximum power point [ohm]	1.8

3.8 Result Analysis

In section 3.5 the calculated result and in section 3.6 the test result is shown. The calculated induced voltage is 8.5 volt but the prototype output voltage is only 5.18 volt. Though in the design the air gap between the rotor and the stator was 1.0mm but while building the generator it was not possible to keep the air gap 1.0 mm as the rotor core material is too much flexible and the pull force of the magnetic pole is very high. Now the air gap is 2.3mm. Using this value in equation 3.7 the air gap flux density is 0.16 T. To get the realistic value of the air gap flux a correction factor of 0.75 is chosen. But the measured air gap flux density is 0.12 T. So the correction factor will be 0.6 other than 0.75. Using the measure air gap flux density in equation in 3.6 and 3.4 the induced voltage is 5.4 volt which is very close to the test data.

3.9 Summary

The first prototyped generator is presented in this chapter. The reasons behind choosing these generator topologies are discussed. While designing the generator a lot of challenges was faced and made compromise on different requirements. The designed generator is described and the test results are presented. An analysis is made on the test result.

Chapter 4

4. SECOND PROTOTYPE

The second prototype is also double rotor internal stator type. The stator of the second prototype is made of printed circuit board (PCB). The design of the generator is described while describing its different parts- rotor, stator, stator winding. The calculated and experimental results are shown. The results are analyzed afterwards.

4.1 Background

According to the earlier research [60], the axial-flux PMSG type is very suitable for low speed applications. In low speed direct driven systems, PM axial-flux generators have proven to be superior to radial-flux generators in many aspects such as high torque/volume ratio, high efficiency and short length [61]. However the axial-gap design cannot take advantage of small air gap because the effective air gap, i.e. summation of mechanical air gap and the height of coil winding, is much greater than the radial-gap design. The reluctance of air is extremely high compared to other materials. Reducing the magnet-to-stator gap improves the efficiency. In addition, it cannot reduce the air gap length because small air gap increases the attractive magnetic force in axial direction, which is directly transmitted to the bearing increases the bearing friction loss.

For conventional AFPM machine, the stator is slotted type as the slotless axial field machines require more magnet material than the slotted one. The slotless machines require a larger diameter due to the additional turns. So the copper loss in the slotless

machine is higher than that of slotted one. Whereas the tooth/slot structure has cogging torque due to the existence of tooth/slot structure. It generally requires some innovative design to reduce the cogging torque [60].

The conventional axial-gap machine has the iron loss due to the alternating magnetic flux in the stator. Iron loss consumes significant amount of power and it increases with the increase of the rotor speed and alternating magnetic flux density [62].

The ironless axial-gap structure can be a good solution as it has no iron loss and no need to concern about the cogging torque reduction. But still the air gap flux density problem reveals. The effective air gap is n times of the diameter of the stator coil in addition to the mechanical clearance and the thickness of resin (where $n = 1 + \text{number of turns}$). It also depends on the height of permanent magnet.

The axial-gap machine using PCB winding is developed to improve the demerits of the conventional machine. The stator coil is replaced by the printed coil of PCB. Since PCB is nonmagnetic material, it has no iron loss in the stator. The magnetic field from the permanent magnets of the two rotors rotates synchronously. This structure has zero cogging torque and there is no unbalanced magnetic force acting on the stator. The effective air gap is the summation of the thickness of the PCB and the mechanical clearance between the rotor and the stator. The PCB is very thin (1/16 inch for a 4 layers PCB) and as the PCB is nonmagnetic material, required mechanical clearance is very small result a very small air gap. This design also prevents the axial magnetic force from being transmitted to the bearing, which decreases mechanical friction loss.

4.2 Design Considerations

The task of an electrical machine design is to determine machine topology, choose necessary materials to be used and decide the size in various sections based on the requirements of power and torque. These required magnetic circuit calculations and verification of the performance equation as the parameters and the dimensions will influence the design result.

Machine design is a synthetic knowledge application of machine theory and machine design experience. In designing second generator, the experience of designing first generator helps a lot. In first prototype, the main design problem was the bending tendency of rotor due to the attraction of force of magnet and the material and thickness of the rotor. With the strong material and thick rotor can help to avoid the bending tendency of the rotor but it will increase the weight of the generator so also the inertia loss.

After designing the first prototype, the objective was to design a generator smaller in size with same number of pole for the same power and torque. For the first design the main challenge was to eliminate the cogging torque, as the cogging torque is the main design problem for a cored stator type PM machine. To eliminate the cogging torque of the first prototype, different techniques was applied which increase the size of the generator. So in case of choosing machine topology the main criteria was a less cogging torque machine geometry.

To avoid cogging torque, coreless stator can be a very good choice. But the coreless geometry poses challenges mostly due to the use of a winding being placed in the air gap and directly exposed to the magnet flux. As a consequence, the coreless

geometry is characterized by extremely low machine inductance and thereby hardly has any constant power range. To overcome this problem, the machine inverter needs to be oversized. The coreless geometry, although doesn't have any core loss, may have significant copper loss due to the induced eddy current in the winding.

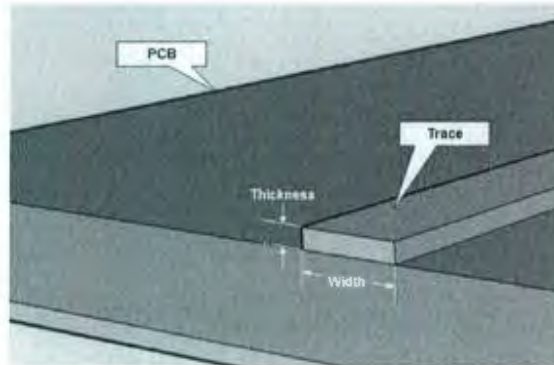


Figure 4.1: PCB board

The PCB stator overcomes the drawback of the conventional coreless geometry. But the printed circuit coil has narrow cross section and therefore high resistance. The lower the trace width (the narrow conducting path as shown in Fig. 4.1) higher the DC resistance and inductance lower the current and higher manufacturing cost. The number of turns and number of coils is also limited by the size of the trace in a specified area. So there should a compromise of trace width that means the current carrying capacity and the number of turns and coils.

4.3 Design

The generator assembly includes two rotor yoke (Upper and lower) incorporate with permanent magnet pole and a printed circuit board stator. The stator is fixed and the rotor is connected with the rotary shaft using hub and bearing.



Figure 4.2: 2D view of the double sided AFPMG with PCB stator

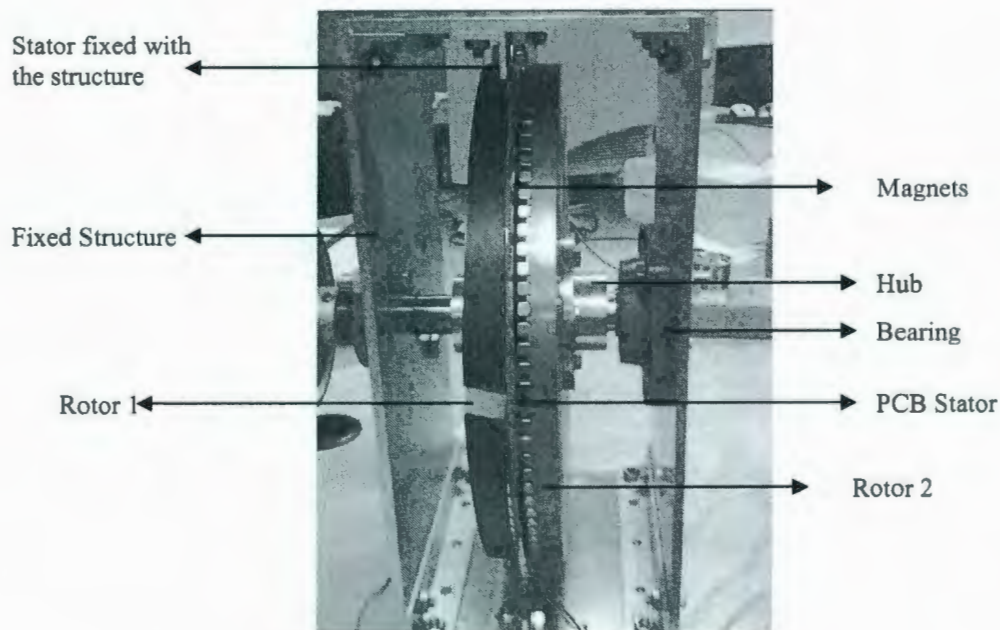


Figure 4.3: The prototyped generator

4.4.1 Rotor

The two rotors are of surface mounted type. The permanent magnets are arranged as shown in Fig. 4.2. This generator configuration is termed as TORUS geometry. In TORUS geometry, the magnets in the two opposite rotor disk may be placed on N-N or N-S arrangements. But the coreless geometry can only be N-S geometry to complete the flux path. The flux direction of this topology is also shown in Fig. 4.2. The two rotors are magnetically and mechanically coupled. The permanent magnets are arranged at equal

angular spacing wherein each pair of magnetic pole pairs is equally magnetized so that the north and the south poles thereof are of equal strength. The yoke is made of mild steel (C-1020) of thickness $\frac{1}{2}$ inches (Fig 4.4). The diameter of the rotor is 300.21mm or 11.82 inch. The magnets are of N-42 grade NdFeB (Table 3.1). The reason for choosing this magnet is depicted in chapter 3.4.1. The magnets are very small in size (Fig. 4.5). While choosing the magnets the criteria was the possible smallest size (1.0 inch \times 0.25 inch \times 0.25 inch) available to keep the size of the generator small that can produce sufficient flux to generate required voltage. The maximum pull force of the magnet is 13.15 lb. Each rotor section has 100 Poles. The theory behind taking large number of pole is explained in chapter 3.4.2. As the size of the magnets is rectangular other than edge shape, the spacing between the magnets is tapered from 0.12 inch to 0.06 inch from the circumference to the centre (Fig 4.6).

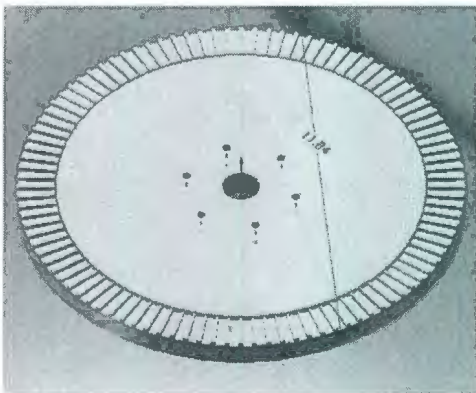


Figure 4.4: Isometric view of the rotor

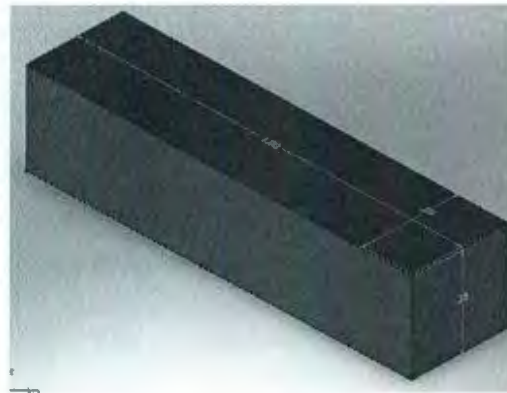


Figure 4.5: 3D view of the magnet with dimensions

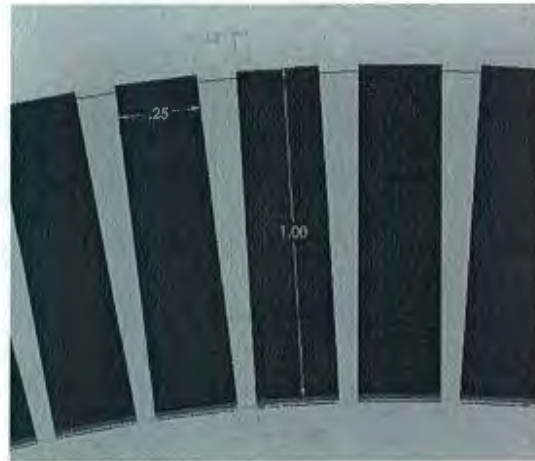


Figure 4.6: The spacing between the magnets

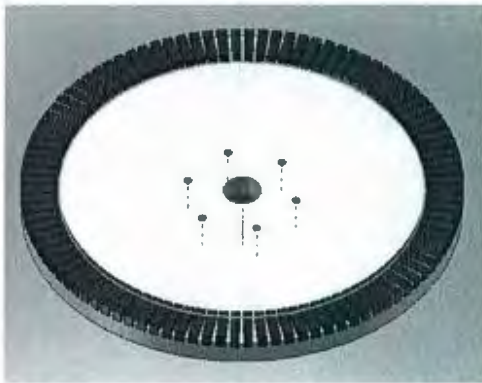


Figure 4.7: Final view of the rotor with magnets

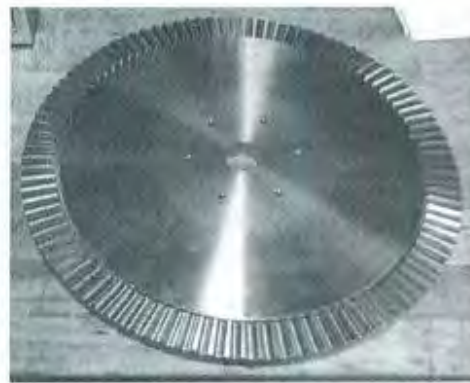


Figure 4.8: The prototype rotor

TABLE 4.1: Rotor Yoke (mild steel C-1020) data

Chemical composition: C=0.20%, Mn=0.45%, P=0.04% max, S=0.05% max			
Property	Value in metric unit		Value in US unit
Density	7.872	$\times 10^3$ kg/m ³	491.4 lb/ft ³
Modulus of elasticity	200	GPa	29000 ksi
Thermal expansion (20 °C)	11.9	$\times 10^{-6}$ °C ⁻¹	6.61 $\times 10^{-6}$ in/(in ³ °F)
Specific heat capacity	486	J/(kg ³ K)	0.116 BTU/(lb ³ °F)
Thermal conductivity	51.9	W/(m ³ K)	360 BTU ³ in/(hr ³ ft ² °F)
Electric resistivity	1.59	$\times 10^{-7}$ Ohm ³ m	1.59 $\times 10^{-8}$ Ohm ³ cm
Tensile strength (hot rolled)	380	MPa	55100 psi
Yield strength (hot rolled)	165	MPa	29700 psi
Elongation (hot rolled)	25	%	25 %
Hardness (hot rolled)	66	RB	66 RB
Tensile strength (cold drawn)	420	MPa	60900 psi
Yield strength (cold drawn)	205	MPa	50800 psi
Elongation (cold drawn)	15	%	15 %
Hardness (cold drawn)	73	RB	73 RB

4.4.2 PCB Stator

The PCB stator winding as used herein refers to a circuit board including a dielectric board (FR-4) with lead wires disposed in different layers of the dielectric board. Fr-4 an abbreviation for Flame Retardant 4 is a type of material used for making PCB. It describes the board substrate, with no copper layer. The FR-4 used in PCBs is typically UV stabilized with tetra functional epoxy resin system. A PCB needs to be an insulator to avoid shorting the circuit, physically strong to protect the copper tracks placed upon it. FR-4 is preferred over cheaper alternatives due to several mechanical and electrical properties. It absorbs less moisture, has greater strength and stiffness.

TABLE 4.2: FR-4 data

Properties	Values
Dielectric constant (permittivity)	4.70 max, 4.35 @ 500 MHz, 4.34 @ 1 GHz
Dissipation factor (loss tangent)	0.02 @1 MHz, 0.01 @ 1 GHz
Dielectric strength	20 MV/mm (500 V/mil)
Surface resistivity (min)	$2 \times 10^5 \text{ M}\Omega$
Volume resistivity (min)	$8 \times 10^7 \text{ M}\Omega \cdot \text{cm}^2/\text{cm}$
Typical thickness	1.25–2.54 mm (0.049–0.100 inches)
Typical stiffness (Young's modulus)	17 GPa (2.5×10^6 PSI; for use in PCBs)
Water absorption	0.10%
Tg (glass transition temperature)	110–200 °C by manufacture and resin system
Thermal Expansion Coefficient	11ppm/K (glass fiber lengthwise)
Thermal Expansion Coefficient	15ppm/K (glass fiber crosswise)
Density	1.91 kg/L

The PCB stator winding is secured to the fixed structure. The PCB winding are at the outer edge of the stator. The stator is tapped at the edge (Fig. 4.9) and the stepped portion is tightly fitted with the structure. But as the PCB is very thin and still flexible, spacer is used to maintain the required equal air gap throughout the circumference.

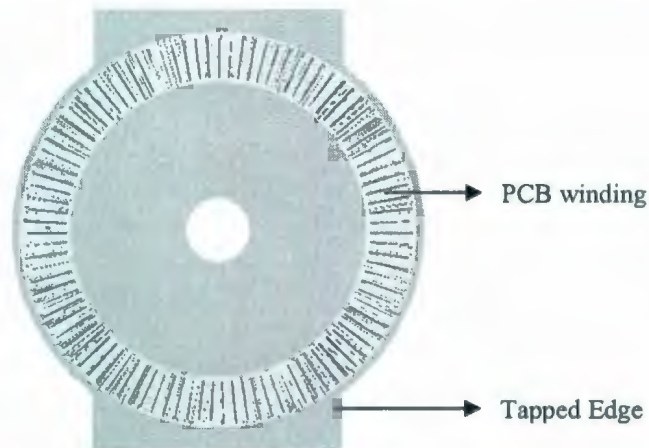


Figure 4.9: The PCB stator

4.4.3 Stator Winding

The coil winding in a conventional axial gap motor is replaced by the printed coil of PCB. The PCB winding can be designed as wave winding and concentric winding (Fig. 4.10) [Special PCB]. The wave winding can be in different shape. The wedge shaped windings offer more surface area than conventional rectangular shape.

The PCB is of 4 layers. In each layer, number of turns is 4 and the number of coil is 100. This is a single phase alternator. In order to increase the voltage of the generator all the coils are connected in series. The choice to increase voltage by connecting all the coils in series is made due to concerns of the current carrying ability of the copper used in the PCB stator. Whereas, to take the advantage of lower resistance, the four stacked stators (4 layers PCB) are wired together in series.

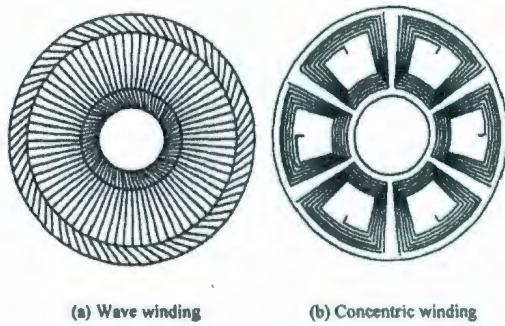


Figure 4.10: PCB winding pattern



Figure 4.11: The designed PCB stator winding

TABLE 4.3: Generator design parameters

Outer radius, r_o [mm]	150
Magnet spacing, τ_f [mm]	0.12
Number of magnets, N_m	100
Number of coils, N_s	4
Number of phases, N_{ph}	1
Magnet thickness, l_m [inch]	0.25
Air gap, δ [mm]	0.7
Dimension of larger magnet (inch)	1.0×0.25×0.25

4.4 Calculated Result

The generator is designed to generate about 12V at a speed of 72rpm. The generator has 100 poles on each of the rotor discs which results in an electrical frequency of 60 Hz at rated speed from equation 3.4.

The number of turns and induced is calculated using the equation 3.5-3.7 as did for the first prototype. The remnant flux density of the magnet is 13 Kilo Gauss (KG) or 1.3 Tesla (T). The length of the magnet in the direction of flux is 0.25 inch or 6.35 mm. The air gap length is the sum of the air gap between the both rotor and the PCB stator and the thickness of the stator. The mechanical clearance between the rotor and the stator is 0.7mm on both sides. The thickness of the stator is 1.6mm. So the total air gap length is

about 3 mm. So from equation (3), the maximum air gap flux density is 0.883T. This would give a rather optimistic value of the air gap flux density. To get a more realistic value an empirical correction factor of 0.75 is used. After correcting the value with the correction factor a maximum air gap flux density of 0.6 T is given.

The area of the magnet is (1.0 inch \times 0.25 inch) 0.25 inch² or 1.6e-4 m². Using the magnet area and the maximum air gap flux density in equation (2) the maximum fundamental flux from each magnet is found 1.1e-4 Weber (Wb). From the equation (2), the number of turns can be calculated to produce required voltage. For this machine 4 turns will induce 12 volt.

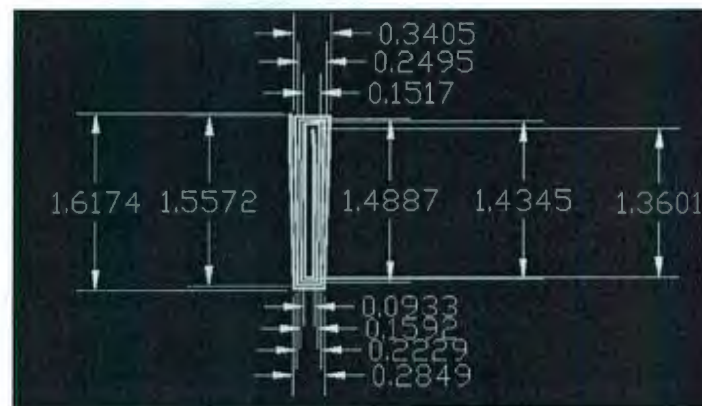


Figure 4.12: The dimension of a single coin with 4 turns

As the trace width of the PCB is 16 mil and the length of each coil calculated from the figure 11 is 13.4403 inch or 34.14 cm. so the resistance of each coil is 0.136 ohm. The coils in 4 layers are connected in parallel and then the 100 coils are connected in series. So the total resistance is 4.3 ohm.

4.5 Test Result

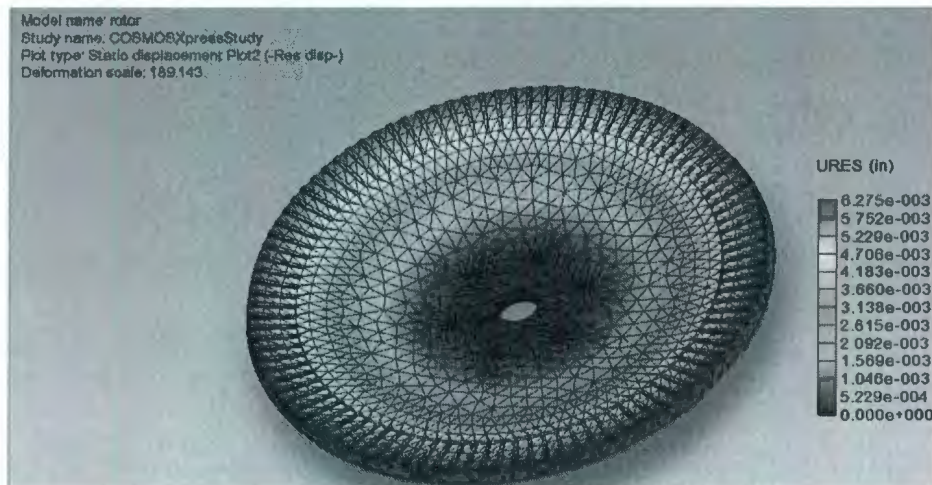
The prototyped generator is built in the technical services of Memorial University of Newfoundland and tested in the lab. For finding the mechanical stability, before building the prototype the generator is simulated by using Solid works software. The prototyped generator is tested and with the data a simplified circuital model of the generator is presented.

4.5.1 Stress and strain test

As the pull force of the magnet is very high, there is a question of using materials and thickness of material for the rotor yoke. While building the first prototype a lot of problem is faced due to the magnetic force and the material and the thickness of the rotor. So the stress and strain of the rotor yoke is tested by FEA using solid works. The maximum stress at the edge is $2e+008$ N/m² and minimum stress at the center is $5e+005$ N/m² (see figure 11). The maximum displacement is $6.275e-003$ inch and the minimum is $5.229e-004$ inch (figure 12).



(a)



(b)

Figure 4.13: (a) Figure 4.13: Static nodal stress of the rotor
(b) Static displacement plot of the rotor

4.5.2 Mechanical parameter test

The main parameters to find out the mechanical characteristic of a generator are inertia and friction. If the inertia and friction is high then the output of the generator will not be satisfactory. These parameters are very important for low speed generator. These parameters are directly related to the torque of the generator. The initial torque for this prototype is zero. The inertia of the generator is also determined following the same procedure and equation as done for the first prototype. The radius of the generator is 0.15m and the density of the mild steel is $7.872 \times 10^3 \text{ kg/m}^3$. The height of each rotor is only 0.0127m. The total inertia of the generator is the sum of inertia of the two rotor and the inertia of the shaft. Inertia of each rotor is 0.106 Kg-m^2 and that of the shaft is 0.001 Kg-m^2 . So the total inertia for the generator is 0.213 Kg-m^2 .

To determine the friction of the generator, the self rotating characteristic of the generator is found (Fig. 4.14). Among the four graphs of Fig. 4.14 two graphs is similar. Taking data from this two graph the friction is determined. These graphs are the linear

portion of an exponential curve which is related to friction and inertia following equation 4.1.

$$N_1 = N_0 e^{-t/BJ} \quad (4.1)$$

Where,

N_1 = rotational speed at time t

N_0 = initial rotational speed

B = friction

J = inertia

The initial rotational speed is not known. Using data from both curves in equation 4.1 friction is determined 0.3.

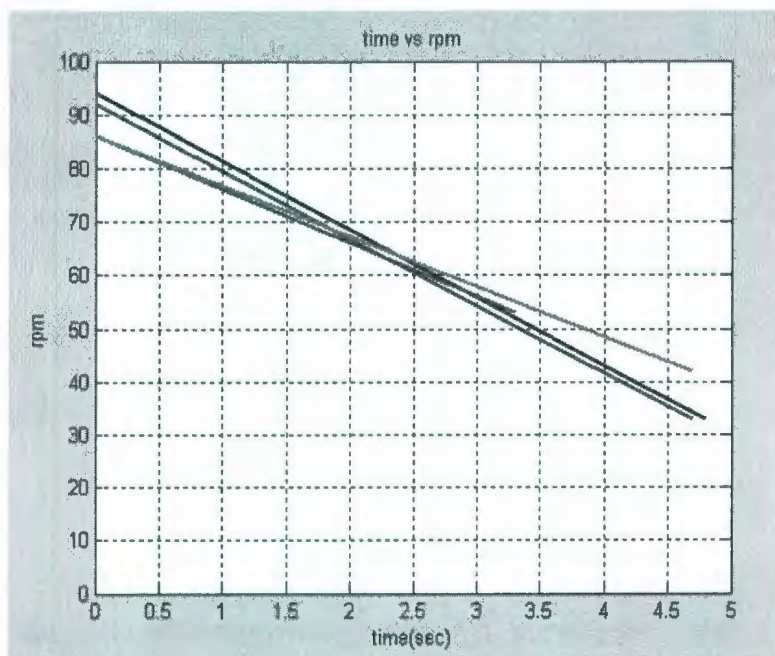


Figure 4.14: Self rotating characteristic

4.5.3 Electrical parameter test

Electrical parameters are required to build the circuit model of the generator. The generator is tested in the lab as did for the first prototype. The internal resistance and

inductance is measured using LCR meter. The test setup is shown in figure 4.15. The test setup contains the generator coupled to a prime-mover. The developed voltage and generating current is recorded through oscilloscope and multimeter for different load (0-20 ohm). The generator is for low speed marine current turbine. So the interest was the characteristic of generator at low speed. Test data is taken at different frequency -20Hz, 25Hz, 30Hz, 35Hz, 40Hz, 55Hz, 60Hz, and 70Hz.

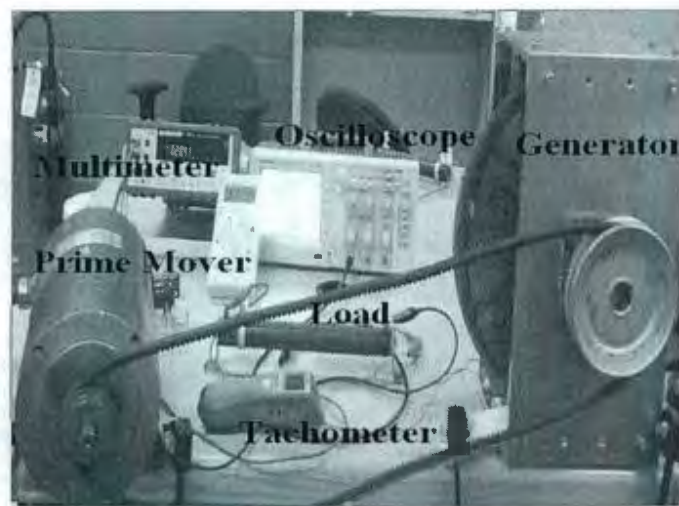


Figure 4.15: Test set up for the prototyped generator

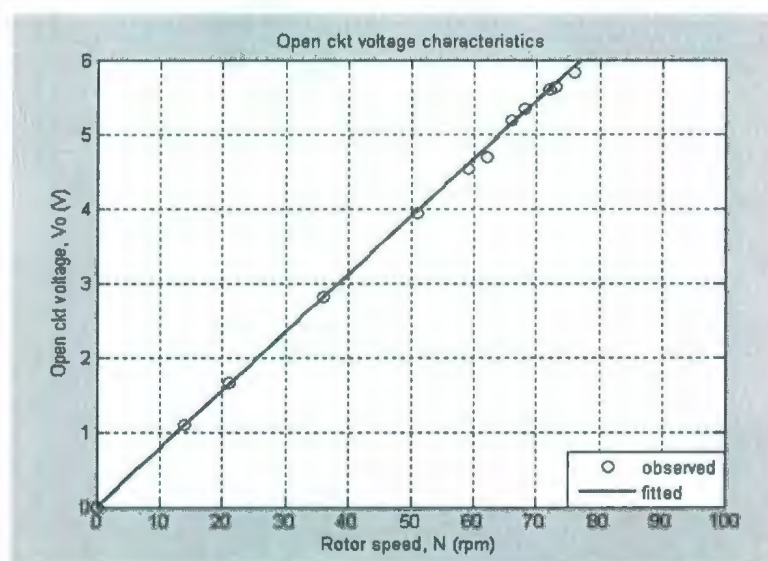


Figure 4.16: Open circuit characteristic curve

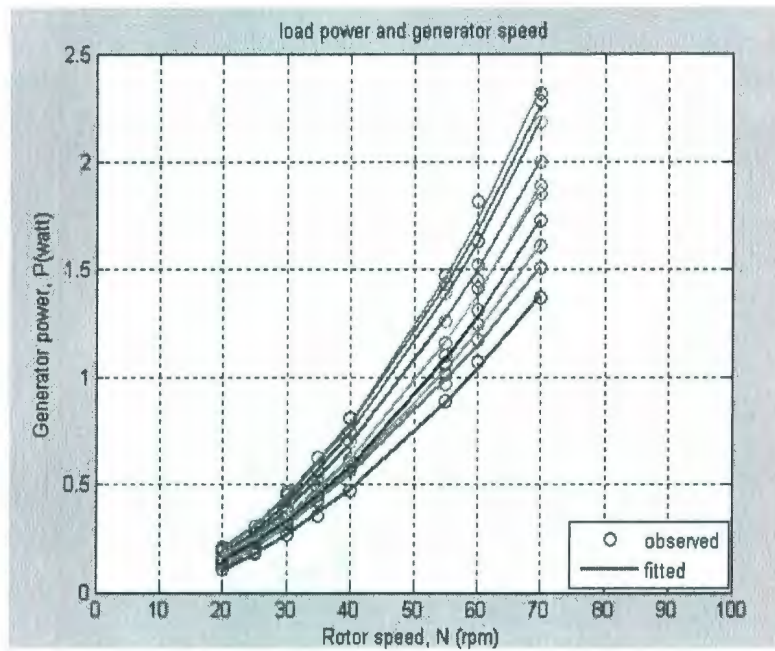


Figure 4.17: Output characteristic for second prototype

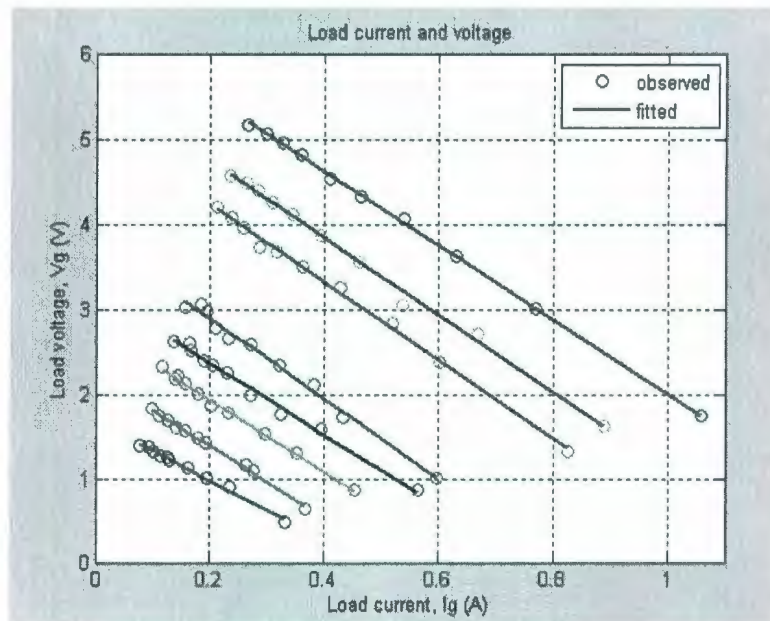


Figure 4.18: load current and voltage for second prototype

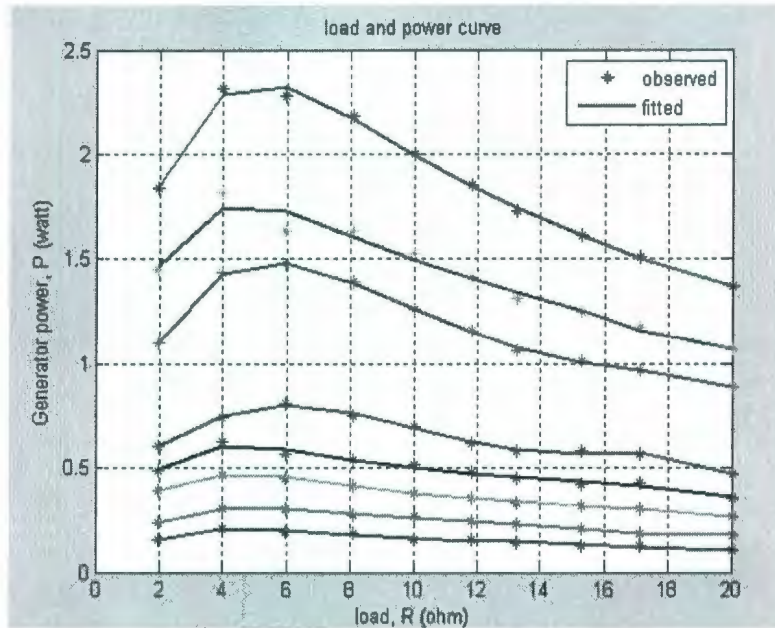


Figure 4.19: Power curve for second prototype

In Fig. 4.16, the open circuit characteristic of the second prototype is shown. In this test no load is connected. At a different frequency voltage induced in the generator terminal is recorded. At designed frequency the open circuit voltage is 5.6 volt. The characteristic is linear with the variation of speed. In Fig 4.17-4.19 the load characteristic is shown. In Fig. 4.18 the induced voltage versus the generating current is shown. Each curve is for a particular frequency at different load. From the curve it is clearly understand the inductance of the generator is very low. From the power curve of the generator (Fig. 4.19) the maximum power point can be traced. Here the maximum power generation occurs between 4 and 5 ohm. It is very difficult to find the exact point. As we measured the internal resistance is 4.4 ohm, so it is clear that maximum power generation will be at 4.3 ohm which is similar to that get from the curve.

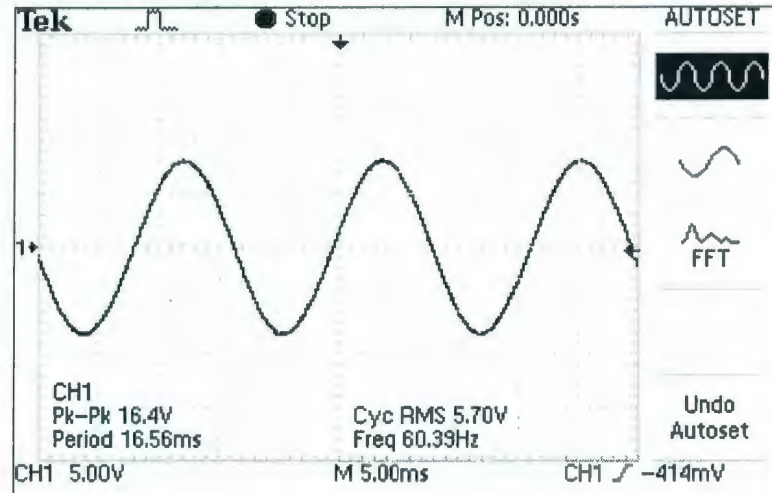


Figure 4.20: The voltage wave form of the second prototype

4.6 Circuital model

As did for the first generator, the circuital model (Fig. 3.17) of the second generator can be build using the same procedure. From the open circuit characteristic the machine constant, λ_m is found 0.078. The internal resistance, $R_g = 1.8$ ohm and internal inductance is $L_g = 216.7 \mu\text{H}$. The R_{null} is found using the curve fitting approach where R_{null} is found $0.0003f^2 + 0.0066f - 0.1107$.

TABLE 4.4: Generator parameters(Second generator)

Internal resistance, R_g , [ohm]	4.4
Internal inductance, L_g [μH]	66.2
Machine constant, λ_m	0.078
No load loss, R_{null} [ohm]	$0.0003f^2 + 0.0066f - 0.1107$
Inertia, J_m [$\text{Kg}\cdot\text{m}^2$]	0.213
Friction, B_m	0.3
Initial torque, T_o [N-m]	0
Open Circuit voltage at 72 rpm [volt]	5.6
Load for maximum power point [ohm]	4.5

4.7 Result Analysis

There is dissimilarity between the calculated and the tested result as happened for the first generator. The reason is also same. The air gap between the PCB stator and the rotor in the design was 0.7mm. But in practical case, we can not make it possible to keep such a small air gap. For this case the rotor is not bending as the rotor is enough strong for the pull force of the magnets. But the thin PCB is flexible and not straight from the centre to the edge. The air gap in prototype generator is 3.3 mm. So from equation 3.7 the maximum flux density is 0.57 T. The correction factor is chosen 0.75. But the measured maximum flux density is 0.35 T. So the correction factor should be 0.6. So the maximum fundamental flux is 0.56×10^{-4} wb. So the calculated induced voltage E_{rms} is 5.9 volt whereas the test data is 5.6 volt which is very close to the calculated result.

4.8 summary

In the second generator the aim was to eliminate the problem faced in designing the first generator. Also the reduction of size and simple construction was the requirement. Though there are some mechanical constrains still reveals in the second prototype but the design requirements were fulfilled.

Chapter 5

5. Conclusion & Future work

5.1. Conclusion

Two PMG for low speed marine current application is designed and developed at Memorial University of Newfoundland. Marine current energy is a promising alternative energy source capable of producing electricity with minimum environmental impact. The ocean current resources still remain predominantly untapped. In this thesis two different type AFPMG has been presented and analyzed for marine current application. The first prototype is cored stator internal stator double sided AFPMG and the second one is PCB stator double sided internal stator type. Two prototyped generators are tested in lab and the mechanical and electrical characteristics of both generators are presented in this paper. Experimental results show that the AFPMG is a very good choice for low speed application like marine current.

The first prototype is very large in size compared to the second prototype. The stator of the generator is made of E-cores. The main drawback of the PMG with cored stator is the cogging torque especially for low speed application. It affects the self starting ability of the generator. So, while designing the first prototype, the main concern was to minimize the cogging torque. Different techniques have been applied to minimize the cogging torque. But the size of the generator can't be optimized. Because of the larger size and weight the inertia and the initial torque of the generator is high. The rotor core was of RENSHAPE material. The RENSHAPE is not strong enough to give a

mechanically rigid structure. To have equal spacing between the both rotor and the stator couple of bearing is used which cause a lots of friction. The winding of the generator is done by hand. This is a very tedious and prone to error. The induced voltage is slightly smaller than that of the second prototype. But as the winding coil size is large for the first prototype, the internal resistance is low. So the generating current is more than that of the second prototype. The result is the larger output power. But the generated voltage has harmonics. The main outcome from this prototype is the larger output power and less cogging torque in cored PMG.

The size of the second prototype is less than the half of the first generator. Also the axial length of the generator is less. As the stator is made of PCB, there is no cogging torque. The initial torque is zero which is an attractive characteristic for low speed marine current application. The inertia and friction of the generator is very small. There is no core in the stator so also core loss. The manufacturing process of the generator is very simple. The voltage induced is larger than that of the first one. But as the PCB winding has a smaller cross section and higher resistance. So the generating current is low and so also the output power. But the waveform of the generated voltage is perfectly sine wave. There is no harmonics. If the generating current is more then cause vibration in PCB. This prototype is a very good choice because of its size, inertia, initial torque, easy manufacturing process, zero cogging torque and magnitude and wave shape of generating voltage though the output power is less.

The first prototype can be used for the application where the larger output is required. The techniques for minimizing the cogging torque can be applied to the other

PMG. The second prototype is suitable for any low speed application because of its zero initial and cogging torque characteristic.

5.2. Future work

The aim of the work was to design a generator to extract few watts electrical energy from marine current. The objective of the work is fulfilled. The work conducted here drew meaningful conclusion and recommendation for the application of both prototypes. The generators are giving expected output and have the desired characteristics. But the both generator has some drawbacks. Future work can be done to overcome constrains and have a better output. To work this area a sound knowledge on three major scientific disciplines, namely electrical engineering, mechanical engineering and material science is required. The following should be further work for anyone who has a great deal of interest in this subject.

- Make the generator totally sealed. If a standard stuffing box is used to couple the generator with the turbine, there will be a possibility to leak and friction will be more. A magnetic clutch might work. The hydrostatic loads due to water pressure should be in consideration.
- Use a suitable material with better rigidity but light in weight for the rotor of the first prototype. The first prototype suffers from the large friction and inertia loss due to its weight and bearings.

- Chose E-cores and magnets of smaller size to reduce the size of the first generator. The first generator is very large and has large inertia.
- Reduce the air gap of the both designed generator. The designed generator had smaller air gap but due to some mechanical constrain maintaining that air gap wasn't possible while developing the generator.
- Optimize the thickness of the rotor of the second prototype. The rotor of the second generator is very heavy and thick, cause more inertia loss.
- Chose PCB with more layers. The second prototype has larger internal resistance and low current. Recently, PCB stators have appeared in the market place. Now 6 layers up to 200oz copper PCB with same thickness as used in second design is available.
- Magnetic gear can be a good choice if the generator is rotate at a very low speed. The efficiency of the magnetic gear is very high.

Great strides will be made in ocean energy harvesting only when the scientific community will pay the proper attention towards this area.

Bibliography

1. International Energy Agency. Share of total primary energy supply in 2003. Technical report, 2003
2. "Status and research and development priorities," IEA/DTI report number FES-R-132 2003
3. J. A. Clarke, G. Connor, A. D. Grant, and C. M. Johnstone, "Regulating the output characteristics of tidal current power stations to facilitate better base load matching over the lunar cycle," *Renewable Energy*, vol. 31, pp. 173-180, 2006.
4. M. Leijon, H. Bernhoff, M. Berg, and O. Ågren, "Economical considerations of renewable electric energy production - especially development of wave energy," *Renewable Energy* vol. 28, pp. 1201-1209, 2003.
5. M. Leijon, A. Rehn, and A. Skoglund, "On the Physics, Engineering and Economics of Renewable Electric Energy Sources," *Submitted to Energy Policy* 2007.
6. Z. Zhang, F. Profumo, and A. Tenconi, "Axial flux versus radial flux PM motors," in *Proc. SPEEDAM*, Capri, Italy, 1996, pp. A4-19-A4-25.
7. R. Qu, "Design and analysis of dual-rotor, radial-flux, toroidallywound, surface-mounted PM machines", Ph.D. Thesis, University of Wisconsin-Madison, Aug, 2002.
8. Gair S, Eastham JF, Profumo F. Permanent magnet brushless d.c. drives for electric vehicles. Int aeagean Conf on Electr Machines and Power Electronics ACEMP'95, Kusadasi, Turkey, 1995, pp. 638-643

9. Spooner E, Chalmers B, El-Missiry MM. A Compact brushless d.c. machine. *Electr Drives Symp EDS'90*, Capri, Italy, 1990, pp. 239-243
10. Lukaniszyn M, Wrobel R, Mendrela A, Drzewoski R. Towards optimization of the disk-type brushless d.c. motor by changing the stator core structure. *Int Conf on Electr Machine ICEM'2000*, Vol pp. 1357-1360.
11. Zhong Z, Lipo TA. "Improvements in EMC performance of inverter-fed motor drives", *IEEE Trans on IA* 31(6):1247-1256, 1995
12. C. C. Jensen, F. Profumo, and T. A. Lipo, "A low loss permanent magnet brushless DC motor utilizing tape wound amorphous iron," *IEEE Trans. Ind. Appl.*, vol. 28, no. 3, pp. 646-651, May/June. 1992.
13. P. Campbell, "Principles of a permanent-magnet axial-field DC machine", *Proc. IEE*, Vol. 121, Dec. 1974, pp.1489-1494.
14. Jahns TM. Motion control with permanent magnet a.c. machines. *Proc IEEE* 82(8):1241-1252, 1994.
15. T. A. Lipo, S Huang and M. Aydin, "Performance assessment of axial flux permanent magnet motors for low noise applications", *Final Report to ONR*, Oct 2000.
16. Metin Aydin, Surong Huang, Thomas A Lipo, " A new axial flux surface mounted permanent magnet machine capable of field control", Conference record of IEEE Industry Applications Society Annual Meeting, 2002, vol. 2, pp. 1250-1257
17. Metin Aydin, Ronghai Qu and Thomas A. Lipo, "Cogging Torque Minimization Technique for Multiple-Rotor, Axial-Flux, Surface-Mounted-PM Motors:

- Alternating Magnet Pole-Arcs in Facing Rotors". Conference record of IEEE Industry Applications Society Annual Meeting, 2003, vol. 1, pp. 555-561
18. T. M. Jahns, W. L. Soong, "Pulsating torque minimization techniques for permanent magnet AC motor drives-a review", IEEE Transaction on Industrial Electronics, Vol.43, No.2, 1996, pp. 321-330.
 19. R. Qu, "Design and analysis of dual-rotor, radial-flux, toroidallywound, surface-mounted PM machines", Ph.D. Thesis, University of Wisconsin-Madison, Aug, 2002.
 20. M. Aydin, "Axial flux surface magnet permanent magnet disc motors for traction drive applications", PhD Preliminary Report, University of Wisconsin-Madison, May 2002.
 21. C. Studer, A. Keyhani, T. Sebastian and S. K. Murthy, "Study in cogging torque in permanent magnet machines", IEEE Industry Applications Society Annual Meeting, 1997, New Orleans, pp. 42-49.
 22. T. Li and G Slemon, "Reduction of cogging torque in permanent magnet motors", IEEE Transactions on Magnetics, Vol. 24, No. 6, Nov 1988, pp. 2901-2903.
 23. Z. Q. Zhu and D. Howe, "Influence of design parameters on cogging torque in permanent magnet machines", IEEE Transactions on Energy Conversion, Vol. 15, No. 4, Dec. 2000.
 24. T. Li and G Slemon, "Reduction of cogging torque in permanent magnet motors", IEEE Transactions on Magnetics, Vol. 24, No. 6, Nov 1988, pp. 2901-2903.

25. Z. Q. Zhu and D. Howe, "Influence of design parameters on cogging torque in permanent magnet machines", *IEEE Transactions on Energy Conversion*, Vol. 15, No. 4, Dec. 2000
26. Metin Aydin, Surong Huang, Thomas A Lipo, " Torque quality and comparison of internal and external rotor axial flux surface-magnet disc machines", *IEEE Trans. Ind. Electron.*, vol. 53, no. 3, pp. 822–830, June. 2006.
27. C. C. Jensen, F. Profumo, and T. A. Lipo, "A low loss permanent magnet brushless DC motor utilizing tape wound amorphous iron," *IEEE Trans. Ind. Appl.*, vol. 28, no. 3, pp. 646–651, May/Jun. 1992.
28. Z. Zhang, F. Profumo, and A. Tenconi, "Axial flux versus radial flux PM motors," in *Proc. SPEEDAM*, Capri, Italy, 1996, pp. A4-19–A4-25.
29. S. Huang, M. Aydin, and T. A. Lipo, "Comparison of (non-slotted and slotted) surface mounted PM motors and axial flux motors for submarine ship drives," in *Proc. 3rd Naval Symp. Elect. Mach.*, Dec. 2000.
30. T. M. Jahns and W. L. Soong, "Pulsating torque minimization techniques for permanent magnet AC motor drives-a review," *IEEE Trans. Ind. Electron.*, vol. 43, no. 2, pp. 321–329, Apr. 1996.
31. C. J. Heine and A. M. El-Antably, *Reluctance and Doubly-Excited Reluctance Motors*, Westinghouse Report submitted to Oak Ridge National Lab., 1984
32. K. Setapati, R. krisnan, "Performance comparisons of radial and axial field, permanentmagnet, brushless machines", Conference record of IEEE Industry Applications Society Annual Meeting, 2000, vol. 1, pp. 228-234

33. A. Cabagnino, M. Lazzari, F. Profumo, A. Tenconi, "A comparison between the axial flux and the radial flux structures for PM synchronous motors.", IEEE Trans. Industry Applications, vol. 38, pp. 1517-1524, Nov.-Dec., 2002.
34. H. Silaghi, V. spoiala, "PM wind generator topologies", Analele Universității din Oradea, Fascicola Electrotehnică, Sectiunea Stiinta Calculatoarelor si Sisteme de Control, Oradea 2006, pp. 118-123.
35. L. Smerlund, J-T. Eriksson, J. Salonen, H. Vihriiila and R. Peda "A Permanent-Magnet Generator for Wind Power Applications." Proc. electromotion'99 July 1999 Patras
36. Chalmers, B.J., Spooner, E., Honorati, O., Crescimbin, F., Caricchi, F. 1997: "Compact Permanent-Magnet Machines," Electric Machines and Power Systems, 1997, Vol.25, pp.635-648.
37. F. Marignetti , V. Delli Colli , P. Cancelliere , M. Scarano, I.Boldea , M. Topor , "A Fractional Slot Axial Flux PM Direct Drive ." IEEE International Conference on Electric Machines and Drives, 2005 , pp. 689-695
38. Y. Chen, P. Pillay, "Axial-flux PM Wind Generator with A SoftMagnetic Composite Core.", Industry Applications Conference, 2005. Fourtieth IAS Annual Meeting. Conference Record of the 2005, vol. 1, pp. 231-237, oct. 2005
39. Ferreira, A.P. Silva, A.M. Costa, A.F. "Prototype of an Axial Flux Permanent Magnet Generator for Wind Energy Systems Applications", European Conference on Power Electronics and Applications, pp.1-9, sept.2007
40. Muljadi, E., Butterfield, C.P., Wan, Y-H. 1999: "Axial Flux Modular Permanent-Magnet Generatorwith a Toroidal Winding for Wind-Turbine Applications," To

- be presented at the 21st American Society of Mechanical Engineers Wind Energy Symposium, Reno, Nevada, January 14–17, 2002
41. Metin Aydin, Ronghai Qu and Thomas A. Lipo, “Cogging Torque Minimization Technique for Multiple-Rotor, Axial-Flux, Surface-Mounted-PM Motors: Alternating Magnet Pole-Arcs in Facing Rotors”. Conference record of IEEE Industry Applications Society Annual Meeting, 2003, vol. 1, pp. 555-561
 42. Dosiek, L. Pillay, P. “Cogging Torque Reduction in Permanent Magnet Machines.”, Industry Applications Conference, 2006. 41st IAS Annual Meeting. Conference Record of the 2006 IEEE, vol. 1, pp. 44-49, Oct. 2006
 43. N. F. Lombard, M. J. Kamper , “ Analysis and Performance of an Ironless Stator Axial Flux PM Machine.”, IEEE Transactions on Energy Conversion, Vol.14, No.4, pp. 1051-1056, Dec, 1999.
 44. G.H. Jang, J.H. Chang “Development of Dual Air Gap Printed Coil BLDC Motor.”, , IEEE Transactions on Magnetics, Vol.35 no.3 pp.1789-1792, May 1999
 45. Hsu, L. Tsai, M. Wu, C. , “Design of a miniature axial flux spindle motor with rhomboidal PCB winding” Magnetics Conference, 2006. IEEE Transactions on Magnetics, vol. 42, No. 10, Oct. 2006
 46. Reed, T. Bakhoun, E. , “ Axial flux permanent magnet alternator using printed circuit board stators.”, Southeastcon, 2008. IEEE, pp. 454-459, April, 2008
 47. F. Caricchi, F. Crescimbin, O. Honorati, G. Bianco, E. Santini, “Performance of coreless-winding axial-flux permanent-magnet generator with power output at

- 400 Hz, 3000 r/min”, IEEE Trans. Industry Applications, vol. 34, pp. 1263-1269, Nov.-Dec., 1998.
48. Metin Aydin, Ronghai Qu and Thomas A. Lipo, “Cogging Torque Minimization Technique for Multiple-Rotor, Axial-Flux, Surface-Mounted-PM Motors: Alternating Magnet Pole-Arcs in Facing Rotors”. Conference record of IEEE Industry Applications Society Annual Meeting, 2003, vol. 1, pp. 555-561
49. K. Rahman, N. Patel, T. Ward, J. Nagashima, F. Caricchi, and F. Drescimbini, “Application of direct drive wheel motor for fuel cell electric and hybrid electric propulsion,” in *proc. IEEE-ias 39th annu. meeting*, oct. 2004, pp. 1420–1426.
50. T. A. Lipo, S. Huang, and M. Aydin, “Performance assessment of axial flux permanent magnet motors for low noise applications,” Wisconsin Electrical Machines and Power Electronics Consortium (WEMPEC), Madison, WI, Final Rep. to ONR, Oct. 2000.
51. S. Huang, M. Aydin, and T. A. Lipo, “Torque quality assessment and sizing optimization for surface mounted PM machines,” in *Proc. IEEE-IAS 36th Annu. Meeting*, 2001, pp. 1603–1610.
52. M. Aydin, S. Huang, and T. A. Lipo, “Optimum design and 3-D finite element analysis of non-slotted and slotted internal rotor type axial flux PM disc machines,” in *Proc. IEEE PES Summer Meeting*, Vancouver, BC, Canada, 2001, pp. 1409–1416.
53. “Design and electromagnetic field analysis of non-slotted and slotted TORUS type axial flux surface mounted disc machines,” in *Proc. IEEE Int. Conf. Elect. Mach. Drives*, Boston, MA, 2001, pp. 645–651.

54. Metin Aydin, "Torque Quality and Comparison of Internal and External Rotor Axial Flux Surface-Magnet Disc Machines", IEEE transactions on industrial electronics, vol. 53, no. 3, june 2006
55. "A New Axial Flux Surface Mounted Permanent Magnet Machine Capable of Field Control" Metin Aydin¹, Surong Huang, Thomas A. Lipo, Industry Applications Conference, 2002. 37th IAS Annual Meeting. Conference Record of the Volume 2, 13-18 Oct. 2002
56. "Cogging Torque Reduction in Permanent Magnet Machines", IEEE transactions on industry applications, vol. 43, no. 6, november/december 2007 1565, Luke Dosiek, Pragasen Pillay
57. "Prototype of an Axial Flux Permanent Magnet Generator for Wind Energy Systems Applications" A. P. Ferreira¹, A. M. Silva², A. F. Costa, Power Electronics and Applications, 2007 European Conference on 2-5 Sept. 2007
58. Khan, M.J. Iqbal, M.T. "Simplified modeling of rectifier-coupled brushless DC generator", International Conference on Electrical and Computer Engineering, 2006. ICECE '06. pp. 349-352, Dec. 2006
59. Khan, M.J. Iqbal, M.T. "Simplified parameter estimation technique of brushless DC generator",
60. Sanjida Moury, M. Tariq Iqbal, "A new approach to minimize the cogging torque of axial flux PMG for under water applications" CCECE conference proceeding, pp- 1167-1171, 2009.

61. Yicheng Chen, pragasen Pillay, and Azeem Khan, "PM wind generator comparison of different topologies," Conference Record of the 2004 IEEE Industry Applications Society, pp 800-807, October 2004
62. J. R. Hendershot and T. J. E. Miller, Design of Brushless Permanent- Magnet Motor: Magna Physics, 1994



